



UNIVERSITAT DE  
BARCELONA

Facultat de Farmàcia  
i Ciències de l'Alimentació

DEGREE FINAL PROJECT  
of the Pharmacy Degree

# DIFFERENT SUBTYPES OF WASTEOSOMES IN THE HUMAN HIPPOCAMPUS

RAQUEL ALSINA PLANELLES

Main scope: Physiology and Physiopathology

Secondary scopes: Immunology & Biochemistry and Molecular Biology

Faculty of Pharmacy and Food Sciences

University of Barcelona

Barcelona, June 2022



This work is licenced under a [Creative Commons](https://creativecommons.org/licenses/by-nc-sa/4.0/) license.





# INDEX

## ABBREVIATIONS

<b>ABSTRACT .....</b>	<b>1</b>
<b>INTEGRATION OF FIELDS .....</b>	<b>3</b>
<b>IDENTIFYING AND REFLECTING ON THE SUSTAINABLE DEVELOPMENT GOALS (SGDs) .....</b>	<b>4</b>
<b>1. INTRODUCTION.....</b>	<b>5</b>
<b>2. OBJECTIVES .....</b>	<b>9</b>
<b>3. MATERIALS AND METHODS.....</b>	<b>10</b>
3.1. SAMPLES .....	10
3.2. EXPERIMENTAL DESIGN .....	10
3.3. METHODS .....	13
3.3.1. Lugol's iodine staining .....	13
3.3.2. PAS staining .....	13
3.3.3. ConA staining .....	14
3.3.4. Double indirect immunofluorescence (hIgM and $\alpha$ -p62).....	14
3.3.5. Digestion with $\gamma$ -amylase .....	15
3.3.6. Image acquisition and processing.....	15
<b>4. RESULTS AND DISCUSSION.....</b>	<b>17</b>
4.1. CHARACTERISATION OF THE HIPPOCAMPAL SECTIONS.....	17
4.2. PRELIMINARY STUDIES .....	19
4.3. DIGESTION STUDIES WITH $\Gamma$ -AMYLASE .....	20
4.3.1. Effect of $\gamma$ -amylase on Lugol's iodine staining of wasteosomes .....	20
4.3.2. Effect of $\gamma$ -amylase on PAS staining of wasteosomes .....	21
4.3.3. Effect of $\gamma$ -amylase on ConA staining of wasteosomes .....	22
4.3.4. Effect of $\gamma$ -amylase on double indirect immunofluorescence (with hIgM and $\alpha$ -p62) of wasteosomes .....	23

4.4. INTEGRATION OF THE RESULTS .....	27
<b>5. CONCLUSIONS .....</b>	<b>30</b>
<b>6. BIBLIOGRAPHY .....</b>	<b>31</b>

## **ANNEXES**

1. HYPOTHESIZED PATHWAY OF THE ELIMINATION OF BRAIN WASTE SUBSTANCES THROUGH WASTEOSOMES
2. THE NATURE OF THE NEO-EPITOPES
3. FEATURES OF OTHER AMYLOLITIC ENZYMES

## **BIBLIOGRAPHY OF THE ANNEXES**

## ABBREVIATIONS

<b>Ab</b>	Antibody
<b>AF</b>	Alexa Fluor
<b>BA</b>	Buffer acetate
<b>BB</b>	Blocking buffer
<b>BB-T</b>	Blocking buffer-Triton
<b>CA</b>	<i>Corpora amylacea</i>
<b>CNS</b>	Central nervous system
<b>ConA</b>	Concanavalin A
<b>ConA-FI</b>	Fluorescein-labelled concanavalin A
<b>CSF</b>	Cerebrospinal fluid
<b>Glc</b>	Glucose
<b>GlcNAc</b>	N-acetylglucosamine
<b>H<sub>2</sub>O<sub>d</sub></b>	Distilled water
<b><sub>h</sub>IgM</b>	Human antibody of immunoglobulin M class
<b>IgM</b>	Antibody of immunoglobulin M class
<b>MBL</b>	Mannose-binding lectin
<b>Man</b>	Mannose
<b>NAb</b>	Natural antibody
<b>NE</b>	Neo-epitopes
<b>PAS</b>	Periodic acid-Schiff
<b>PBS</b>	Phosphate-buffered saline
<b>p62</b>	Sequestosome-1 or ubiquitin-binding protein p62
<b>RT</b>	Room temperature
<b>TEM</b>	Transmission electron microscopy
<b>Ubi</b>	Ubiquitin
<b><math>\alpha</math>-p62</b>	Monoclonal mouse antibody of isotype IgG <sub>2a</sub> against the ubiquitin-binding protein p62



## ABSTRACT

### Different subtypes of wasteosomes in the human hippocampus

Wasteosomes (also known as *corpora amylacea*) are polyglucosan bodies that amass waste substances. They are generated in the central nervous system during normal aging and neurodegenerative processes, then extruded into the cerebrospinal fluid and finally phagocytised by macrophages in the cervical lymph nodes. In this work we study the possible existence of different wasteosomes depending on their location in the human hippocampus. We performed staining techniques combined with digestion with  $\gamma$ -amylase. These techniques were Lugol's iodine, periodic acid-Schiff and concanavalin A staining, and a double indirect immunofluorescence to detect the neo-epitopes and the protein p62. Results showed there are two subtypes of wasteosomes with respect to their behaviour towards  $\gamma$ -amylase and their content in neo-epitopes and protein p62. Wasteosomes in the inner areas of the hippocampus contained more protein p62, less neo-epitopes, and had a less resistant polymerised structure towards  $\gamma$ -amylase. Conversely, wasteosomes in the peripheral areas of the hippocampus contained less protein p62, more neo-epitopes, and had a more resistant polymerised structure towards  $\gamma$ -amylase. The differences observed could be related to different maturation stages. Wasteosomes in the inner areas could have a less phosphorylated and a more branched amylopectin-like polymer structure, whereas wasteosomes in the peripheral areas could have a mainly phosphorylated and a less branched amylose-like polymer structure. These findings reinforce that wasteosomes are involved in the elimination of brain waste substances, for which reason they undergo a maturation process during which composition and structural changes may occur.

**Key words:** *corpora amylacea*, wasteosomes,  $\gamma$ -amylase, human hippocampus.

## RESUM

### Diferents subtipus de *wasteosomes* en l'hipocamp humà

Els *wasteosomes* (o *corpora amylacea*) són cossos de poliglucosa que acumulen substàncies de rebuig. Són generats a nivell del sistema nerviós central durant l'envelliment i processos neurodegeneratius, més tard extruïts al líquid cefalorraquidi i finalment fagocitats per macròfags en els ganglis limfàtics cervicals. En aquest treball estudiem la possible existència de diferents *wasteosomes* segons la seva localització en l'hipocamp humà. Vam aplicar tècniques de tinció combinades amb la digestió amb  $\gamma$ -amilasa. Aquestes tècniques van ser les tincions amb Lugol-iodina, àcid periòdic-Schiff i concanavalina A, i una doble immunofluorescència indirecta per a detectar els neo-epítops i la proteïna p62. Els resultats van mostrar l'existència de dos subtipus de *wasteosomes* en relació al seu comportament enfront la  $\gamma$ -amilasa i al seu contingut en neo-epítops i proteïna p62. Els *wasteosomes* en zones internes de l'hipocamp contenen més proteïna p62, menys neo-epítops, i una estructura polimèrica menys resistent a la  $\gamma$ -amilasa. En canvi, els *wasteosomes* en zones perifèriques contenen menys proteïna p62, més neo-epítops, i una estructura polimèrica més resistent a la  $\gamma$ -amilasa. Les diferències observades es podrien relacionar amb diferents estats de maduració. Els *wasteosomes* en zones internes tindrien una estructura menys fosforilada i més ramificada, semblant a la de l'amilopectina, mentre que els *wasteosomes* en zones perifèriques la tindrien majoritàriament fosforilada i menys ramificada, semblant a la de l'amilosa. Aquestes troballes reafirmem que els *wasteosomes* estan implicats en l'eliminació de substàncies de rebuig del cervell, motiu pel qual experimentem un procés de maduració durant el qual la seva composició i estructura canviarien.

**Paraules clau:** *corpora amylacea*, *wasteosomes*,  $\gamma$ -amilasa, hipocamp humà.

## INTEGRATION OF FIELDS

The present Degree Final Project includes *Physiology and Physiopathology* as the main scope. The secondary scopes involved in the study are *Immunology* and *Biochemistry and Molecular Biology*.

### - **Physiology and Physiopathology:**

This work is focused on the study of human brain wasteosomes and the possible existence of different subtypes. Wasteosomes are polyglucosan bodies generated in the central nervous system during normal aging and neurodegenerative processes. It is presumed they may be involved in the cleaning of brain waste substances. For this reason, a detailed characterisation of these bodies could be of help in a better understanding of their development and their relation to neurodegenerative diseases.

Our long-term goal is to determine the physiological or physiopathological function of wasteosomes. This knowledge could allow the use of wasteosomes as a diagnosis tool, since we speculate that they may contain clinical markers of brain diseases. Such use has been hypothesised to be applicable in the future seeing that it is possible to obtain and study wasteosomes from lumbar puncture samples.

### - **Biochemistry and Molecular Biology:**

The purpose of this work is to achieve a better understanding of the development and the biochemical features of wasteosomes. Considering that wasteosomes are mainly formed by polymerised hexoses and that their neo-epitopes appear to be of carbohydrate nature, combining staining methods based on the interaction of some reagents and carbohydrates, with digestion with  $\gamma$ -amylase, may provide new information. Therefore, notions of biochemistry and molecular biology will be of help to our purpose.

### - **Immunology:**

The purpose of this work is to characterise in more detail wasteosomes. For this reason, the recognition of components contained in wasteosomes with primary and secondary antibodies by using immunofluorescence techniques may be useful for the study of their structure and development. In addition, the neo-epitopes of wasteosomes are recognised by natural antibodies of the immunoglobulin M class. Such interaction links these bodies to the innate immune response and could be implicated in their phagocytosis and, consequently, in the physiological or physiopathological response in charge of the elimination of brain waste substances. Therefore, notions of immunology will be of help to our purpose.

# IDENTIFYING AND REFLECTING ON THE SUSTAINABLE DEVELOPMENT GOALS (SDGs)



*The 17 Sustainable Development Goals included in the 2030 Agenda, approved in 2017 by the United Nations, as a plan of action for the three dimensions of the sustainable development: the economic, the social, and the environmental.*<sup>1</sup>

The SDGs<sup>2</sup> addressed in this work are related to the improvement of health and well-being in the world, the equality between women and men, the sustainable management of water, and the enhance of innovation.

To start, improved knowledge of the development, structure, and function of wasteosomes could be useful to use these bodies as diagnosis tools for neurodegenerative diseases. This can be connected to **target 3.D of SDG 3** “*Strengthen the capacity of all countries, in particular developing countries, for early warning, risk reduction and management of national and global health risk*”<sup>2</sup>. Nonetheless, no indicator has been found for this target. Secondly, considering our objective is to obtain information from samples of men and women, without making any difference, the work could be related to **target 5.1 of SDG 5** “*End all forms of discrimination against all women and girls everywhere*”<sup>2</sup>, which is valued by the indicator 5.1.1 “*Whether or not legal frameworks are in place to promote, enforce and monitor equality and non-discrimination on the basis of sex*”<sup>2</sup>. Next, the reagent management according to the guidelines of the *Unitat de Laboratoris Docents* of the Faculty of Pharmacy and Food Science follows the **target 6.3 of SDG 6** “*By 2030, improve water quality by reducing pollution, eliminating dumping and minimizing release of hazardous chemicals and materials, halving the proportion of untreated wastewater and substantially increasing recycling and safe reuse globally*”<sup>2</sup>, for which the indicators 6.3.1 “*Proportion of wastewater safely treated*”<sup>2</sup> and 6.3.2 “*Proportion of bodies of water with good ambient water quality*”<sup>2</sup> can be used. Finally, this study discloses the necessity to enhance scientific research, as explained in **target 9.5 of SDG 9** “*Enhance scientific research, upgrade the technological capabilities of industrial sectors in all countries, in particular developing countries, including, by 2030, encouraging innovation and substantially increasing the number of research and development workers per 1 million people and public and private research and development spending*”<sup>2</sup>. For this last target, remarkable not only in neurosciences but in scientific research in general, there are the indicators 9.5.1 “*Research and development expenditure as a proportion of gross domestic product*”<sup>2</sup> and 9.5.2 “*Researchers (in full-time equivalent) per million inhabitants*”<sup>2</sup>.

---

<sup>1</sup> European Commission. Sustainable Development Goals [Internet]. Belgium: European Commission; 2022 [cited 14 February 2022]. Available in: [https://ec.europa.eu/international-partnerships/sustainable-development-goals\\_hr?2nd-language=es](https://ec.europa.eu/international-partnerships/sustainable-development-goals_hr?2nd-language=es)

<sup>2</sup> United Nations. Global indicator framework for the Sustainable Development Goals and targets of the 2030 Agenda for Sustainable Development. Transforming Our World: The 2030 agenda for sustainable development [Internet]. New York: United Nations Statistics Division Development Data and Outreach Branch; c2022 [cited 14 February 2022]. Available in: <https://unstats.un.org/sdgs/indicators/indicators-list/>

## 1. INTRODUCTION

The term *corpora amylacea* (CA) was firstly introduced by Virchow, in 1854, after finding similarities between these bodies and starch (1). However, these bodies, which are polyglucosan structures (2,3), had already been described by J.E. Purkinje. In 1837, the physiologist and anatomist noticed the presence of granular bodies in brains from elderly people (4). Certainly, CA have been described by many scientists through history, but for a long time they have been considered irrelevant. Nowadays, it is known CA tend to accumulate in central nervous system (CNS) during aging and, remarkably, during neurodegenerative processes such as Alzheimer's disease, Parkinson's disease, Huntington's disease, and frontotemporal dementia, among others (5,6). Therefore, these bodies could be a new key point in the study of age-related and neurodegenerative brain processes (7).

CA are intracellular spherical bodies, although sometimes rather oval or elongated, with a diameter that ranges between 2  $\mu\text{m}$  and 20  $\mu\text{m}$ , while sometimes larger. Their surface is smooth, but when stained, concentric laminated or target patterns can be seen. In fact, the presence of such concentric rings could be explained by considering CA undergo different growth stages (2). In ultrastructural studies with transmission electron microscopy (TEM), correlative serial block-face scanning electron microscopy and transmission electron tomography, CA appear to be formed by short linear fibres densely packed, sometimes concentrated in the centre, and surrounded by a membrane (Fig. 1) (8,9).

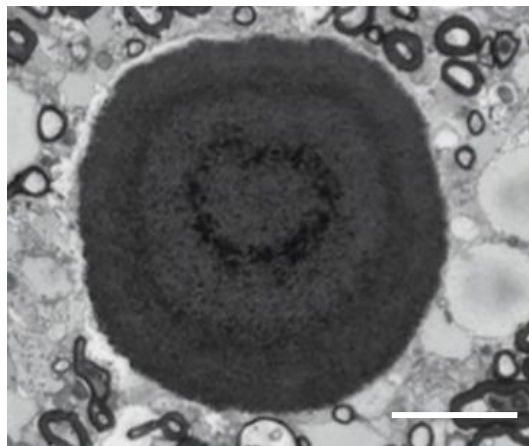


*Figure 1: Human hippocampal CA visualised by serial block-face scanning electron microscopy showing concentric layers. Scale bar: 5  $\mu\text{m}$ . Adapted from (9).*

The origin and function of CA have been controversial for some time. While some scientists have stood up for a neuronal origin, it is more likely CA proceed from fibrillar astrocytes. Ultrastructural TEM studies and immunofluorescence techniques show CA

are found in the cytoplasm of cells containing glial fibrillary acidic protein, which is expressed by astrocytes. In addition, these studies show that cellular debris, degenerated mitochondria, and membranous vesicles, all of which increase with ageing and oxidative stress, accumulate near CA (8,10–12). It has been proposed CA are generated by astrocytes entrapping and accumulating waste substances from neuronal, glial and blood origin (2,6), and even from microbial and fungal infections (13). Therefore, CA may constitute another physiological or physiopathological system to eliminate cellular waste besides the ubiquitin (Ubi) proteasome system and the phagosome/lysosome pathway (12). Moreover, CA components vary depending on where these bodies are generated (12). This study is focused on human brain CA, but CA can also be found in heart, liver, prostate, lung, thyroid, and muscle (2). Besides, since the term *amyloid*, which is used to refer to starch-like structures such as CA, can lead to confusion with fibrillary proteins, which are not always present in CA (10), a recent study proposes to rename CA as “wasteosomes” (12). Hence, from now on, we will talk about wasteosomes.

Regarding the function of wasteosomes as waste containers, there are some facts supporting this theory. In the first place, it is known they are polyglucosan bodies with polymerized hexoses, mainly glucose (Glc), as basic components. In 1969, Sakai *et al.* conducted the first isolation and preliminary characterization studies, in which they concluded wasteosomes contain 68,4 % hexoses, 8,1 % proteins and a remaining 23,5 % with, among other unidentified components, phosphate groups (3). Therefore, it is of no surprise these bodies incorporate glycogen synthase, an indispensable enzyme for the formation of Glc polymers, located mainly in the periphery. In addition, Sakai *et al.* concluded that the polymerized Glc<sub>s</sub> have similar features with amylopectin and glycogen (3). Regarding the protein content, wasteosomes contain Ubi and Ubi-binding protein p62 (p62; also known as sequestosome-1), both of which are associated with the signalling and degradation of waste substances. While Ubi can be found in the periphery of wasteosomes, it tends to concentrate in the centre, and p62 is found mainly in the periphery. Considering the distribution of glycogen synthase, Ubi and p62, it can be hypothesised that polymerized hexoses are formed in the periphery of wasteosomes, while ubiquitinated waste substances are entrapped, whereas the central part is where these waste substances will remain (10). This would explain the presence of concentric rings that appear when wasteosomes are stained. In the same way, ultrastructural TEM studies show wasteosomes are different depending on their maturation state. Most of the wasteosomes are formed of short linear fibres that are densely packed, while a few of them are less organized, likely due to their immature state (Fig. 2) (8). Finally, with respect to the phosphate content, digestion studies with amylolytic enzymes suggest phosphate groups could be found esterified with Glc units (3). These phosphate groups are known to interfere directly with the activity of amylolytic enzymes and indirectly due to their modulation effect on glycogen branching pattern and solubility. As a result, a higher phosphate content is related to a lower accessibility of amylolytic interacting enzymes (14).

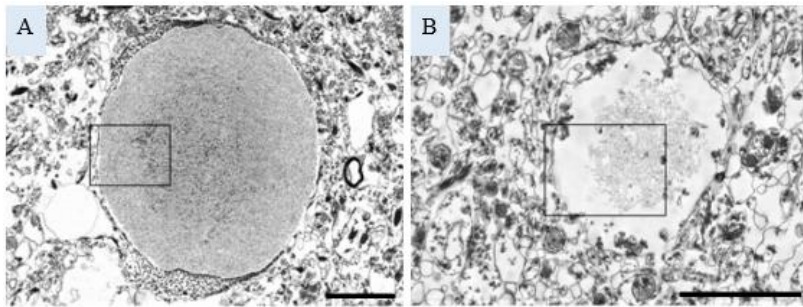


*Figure 2: TEM images of hippocampal mature (A) and immature (B) wasteosomes from human brain. Scale bar: 3  $\mu\text{m}$  (A) and 2  $\mu\text{m}$  (B). Adapted from (8).*

In the second place, wasteosomes can be found in any part of the brain, but they tend to accumulate noticeably in the hippocampus, generally in the following bordering areas: perivascular, periventricular and subpial regions (3). On one hand, periventricular and subpial regions are close to the ventricles and the subarachnoid space respectively, which both contain cerebrospinal fluid (CSF). On the other hand, the glymphatic system, a waste clearance system in the CNS, drains the interstitial fluid into perivenous spaces and later to the subarachnoid space (15,16). Therefore, it is reasonable to think wasteosomes are extruded from the brain to the CSF (2,11). Such fact, supported by the presence of matrix-metalloproteinase-2 inside wasteosomes, a protein which executes extracellular remodelling (10), has been demonstrated by the finding of wasteosomes in post-mortem intraventricular CSF (17). Furthermore, the recently rediscovered meningeal lymphatic system (18) has made it possible to explain how macromolecules and wasteosomes from brain present in CSF can get to the cervical lymph nodes. It would be in the cervical lymph nodes where wasteosomes are phagocytised by macrophages, a process probably mediated by different paths. Extra information about the hypothesized pathway of the elimination of brain waste substances through wasteosomes can be found in [Annex 1](#).

Finally, it must be highlighted that Augé *et al.* demonstrated wasteosomes contain neo-epitopes (NE), in other words, epitopes formed *de novo* in physiological and physiopathological situations (19,20). These NE are recognised by antibodies ( $\text{Ab}_s$ ) of immunoglobulin M class (IgM) ([Fig. 3](#)) (7), which once again corroborates the function of wasteosomes as waste containers, given that  $\text{IgM}_s$  are known to participate in the clearance of misfolded proteins, dying cells and other altered structures, to avoid inflammation and autoimmunity (21). The NE can be found in the whole structure of wasteosomes, as proved by staining of serially cut semi-thin sections of 500 nm - 1  $\mu\text{m}$  thickness. However, when staining sections of 60  $\mu\text{m}$  thickness, the staining only appears in the peripheral area of wasteosomes. This happens because the densely packed short linear fibres of wasteosomes do not allow the penetration of  $\text{IgM}_s$  (8). In the study of Augé *et al.*, it was also checked that, as expected, the NE are likewise recognised by sera from different mammal species and serum from human umbilical cord (7). The explanation to such results is that the  $\text{IgM}_s$  binding NE are natural  $\text{Ab}_s$  ( $\text{NAb}_s$ ).  $\text{NAb}_s$  are usually interspecific because they have been selected through evolution and their production does not precise antigenic stimulation (21). They can be of the IgM, immunoglobulin G or immunoglobulin A classes (22) and their selected restricted binding

repertoire results from the germline encoded VH and VL genes (23). The main NAb<sub>s</sub> found in human sera are human IgM<sub>s</sub> (hIgM), generally produced by B-1 cells (21,24,25). NAb<sub>s</sub> participate in the immune homeostasis and are characterised as Ab<sub>s</sub> with low affinity, high avidity, and multi-reactivity against a restricted repertoire of self-antigens selected through evolution (22,26), which includes carbohydrates, glycoproteins, phospholipids, and nucleic acids (27). Therefore, the low affinity is compensated by IgM<sub>s</sub> being pentameric and multi-reactive (28). In relation to the interaction between hIgM<sub>s</sub> and the NE of wasteosomes, it must be noted that hIgM<sub>s</sub> do not cross the blood-brain barrier because of their size (7), so the interaction between them can only be explained thanks to the now confirmed extrusion of wasteosomes.

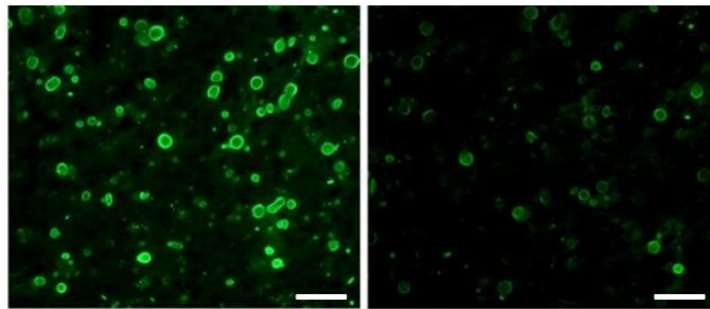


*Figure 3: Human hippocampal sections from an Alzheimer's disease donor immunostained with two different human blood plasmas in the first incubation and Ab<sub>s</sub> against hIgM ( $\alpha$ -hIgM) ( $\mu$  chain specific) conjugated to a fluorophore in the second incubation. Scale bar: 50  $\mu$ m. Adapted from (7).*

Although it would be interesting to uncover the exact composition of the NE, there are still other loosed ends regarding human brain wasteosomes. For this reason, it is needed to continue with the characterisation of these bodies, especially regarding their polyglucosan framework. Extra information about the nature of the NE of wasteosomes can be found in [Annex 2](#). Back in 1969, Sakai *et al.* executed the first digestion studies with amyolytic enzymes. Such studies showed that  $\gamma$ -amylase (also known as amyloglucosidase) and  $\alpha$ -amylase reduced the intensity of staining techniques based on sugar binding, whereas  $\beta$ -amylase and phosphorylase had minimal effect. These results suggest wasteosomes contain polymerized hexoses with  $\alpha$ -1:4 and  $\alpha$ -1:6 linkages. It was also noted that digestion with amyolytic enzymes was difficult due to the highly aggregated structure of wasteosomes. In addition, Sakai *et al.* used Lugol's iodine staining, results of which suggested wasteosomes contain long and short Glc chains, since some of them turned purplish while some others turned brown. All in all, Sakai *et al.* concluded wasteosomes contain aggregates of polymerized hexoses that have similar features with amylopectin and glycogen (3). Nevertheless, Sakai *et al.* mainly focused on the study of isolated wasteosomes, for which reason differences depending on the location of wasteosomes were not considered. Furthermore, the purification treatments applied to isolate the wasteosomes could have interfered with their results. Accordingly, we aim to find more information, or corroborate the already known, by conducting digestion studies with  $\gamma$ -amylase and analysing the effect in different areas of the human hippocampus.

## **2. OBJECTIVES**

The main objective of the present work is to find out if there exist differences between wasteosomes when located in different areas of the human hippocampus. For our purpose, the study will combine different staining techniques with the digestion effect of  $\gamma$ -amylase in wasteosomes located in inner and peripheral areas of human hippocampal sections.

More knowledge about these bodies will help in the understanding of their development and role on the hypothesised physiological or physiopathological pathway for the elimination of brain waste substances through wasteosomes.

### 3. MATERIALS AND METHODS

#### 3.1. SAMPLES

Post-mortem cryo-preserved hippocampal sections (thickness of 6  $\mu\text{m}$ ) from brain disease patients were provided by the Neurological Tissue Bank of the Biobanc - Hospital Clínic - IDIBAPS (Barcelona, Spain). Samples were stored at  $-80\text{ }^{\circ}\text{C}$  until their use. Medical data on donors is specified in [Table 1](#).

*Table 1: Medical data on the donors of the hippocampal samples: case number, neuropathological characterization (post-mortem), clinical diagnose, sex (F, female; M, male), age and post-mortem delay (HH:MM, hours:minutes).*

Case number	Neuropathological characterization	Clinical diagnosis	Sex	Age	Post-mortem delay (HH:MM)
1	Alzheimer's disease	Control	M	86	7:15
2	Alzheimer's disease	Alzheimer's disease	M	87	5:00
3	Vascular encephalopathy	Dementia	M	80	10:00

Cases 1, 2 and 3 were used for the main part of the research, which corresponds to the staining techniques combined with digestion studies with  $\gamma$ -amylase, whereas only case 1 was used for the preliminary tests carried out to set on the experiments. As can be guessed from [Table 1](#), donors were chosen among elderly people with a neuropathological diagnosis, because of their higher number of wasteosomes, and with the lowest post-mortem delay, to have the best possible tissue preservation. Due to our selection criteria commented above, we were only able to work with men hippocampal samples. However, this is an initial study, and our intention is to extend it with future studies with a higher number of samples and including both genders.

This study has been approved by the Bioethical Committee of the University of Barcelona and all experiments involving human samples have been conducted following proper guidelines and regulations.

#### 3.2. EXPERIMENTAL DESIGN

The study was divided in two main parts. Firstly, initial Lugol's iodine ( $\text{I}_2 + \text{KI}$ ) staining, periodic acid-Schiff (PAS) staining, concanavalin A (ConA) staining and immunofluorescence detection of the NE and the p62 were conducted to make sure protocols were adequate for the study of wasteosomes. These preliminary studies also included checking the functionality of  $\gamma$ -amylase and developing and optimising the corresponding digestion protocol. Secondly, digestion studies with  $\gamma$ -amylase followed

by Lugol's iodine staining, PAS staining, ConA staining and immunofluorescence detection of the NE and the p62 were carried out. The basis of the mentioned techniques is detailed after the illustration of the experimental design (Fig. 4).

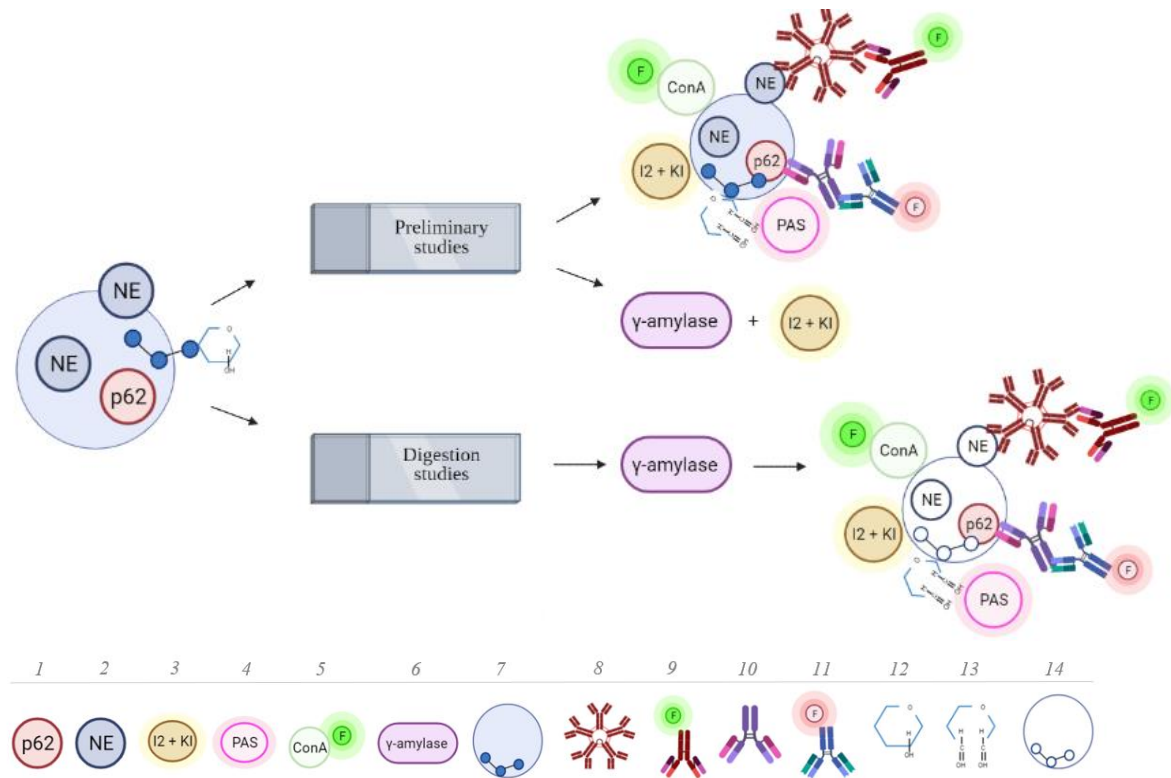


**Figure 4:** Diagram of the experimental design and its legend. **1**, protein p62; **2**, neo-epitopes; **3**, Lugol's iodine staining; **4**, PAS staining; **5**, ConA staining with ConA labelled to a fluorophore; **6**, digestion with  $\gamma$ -amylase; **7**, wasteosome with a sugar chain; **8**,  $n$ IgM; **9**, Ab against  $n$ IgM ( $\mu$  chain specific) labelled to a fluorophore; **10**, IgG<sub>2a</sub> against p62; **11**, Ab against the IgG<sub>2a</sub> against p62 labelled to a fluorophore; **12**, reduced sugar from the sugar chain; **13**, oxidised sugar from the sugar chain; **14**, suggested representation of a wasteosome after treatment with  $\gamma$ -amylase. Illustration created by the author with © BioRender 2022.

**Lugol's iodine staining** ( $I_2 + KI$ ) is used to detect starch and glycogen, for which reason it can be useful to characterize starch-like polyglucosans. The colour of the staining varies depending on the structure. Amylose, which consists of linear Glc units with  $\alpha$ -1:4 glycosidic bonds, stains in deep blue-black due to the formation of a stable complex with triiodide. Amylopectin, which consists of linear Glc units with  $\alpha$ -1:4 glycosidic bonds and ramifications with  $\alpha$ -1:6 glycosidic bonds, is not able to create a stable complex with triiodide and stains in reddish-purple colour. Glycogen, which is shorter and has more ramifications than amylopectin, barely stains with Lugol's iodine (3,29). Added to the fact that phosphorylation reduces the activity of amyolytic enzymes, it can be said that the more lineal and phosphorylated is a polyglucosan, the darker it stains with Lugol's iodine staining. Given that wasteosomes are polyglucosan bodies, they can be stained by Lugol's iodine. In fact, Sakai *et al.* proposed wasteosomes contain long Glc chains mixed

with shorter ones that resemble amylopectin and glycogen because they stain in a purplish-brown colour (3).

PAS staining is a histochemical staining used to visualize carbohydrates. The periodic acid acts in the 1,2-glycol linkage (1-amino-2-hydroxy linkage is also possible) and oxidises the hydroxyl groups to the corresponding aldehyde groups (-CHOH-CHOH- → RCHO + RCHO). Next, the aldehyde groups react with the Schiff reagent, resulting in a purple complex (30). Bearing in mind wasteosomes contain 68,4 % polymerised hexoses, they can be stained by PAS.

ConA staining is based on the use of the lectin obtained from *Canavalia ensiformis*, a soluble carbohydrate-binding protein. Lectins are classified in families according to their carbohydrate-recognition domains, which usually recognise terminal glycan groups. ConA precipitates with certain  $\alpha$ -glucans that contain mannose (Man), Glc, fructose and N-acetylglucosamine (GlcNAc) (31). Since wasteosomes contain high amounts of Glc and other saccharides, ConA allows the detection of wasteosomes. However, to use ConA as a marker of wasteosomes, it is necessary to conjugate the protein with an enzyme or a fluorophore which will allow the later recognition in the microscope.

Double indirect immunofluorescence with  $_h$ IgM and an Ab against p62 ( $\alpha$ -p62) can be used to visualise the NE and the p62 of wasteosomes. Firstly, primary Ab<sub>s</sub> bind to their targets, the NE and p62. Secondly, secondary Ab<sub>s</sub> bound to a fluorophore bind to the primary Ab<sub>s</sub> (32). In order to avoid specificity problems, secondary Abs are directed against the Fc region of the primary Ab<sub>s</sub> and are isotype specific.

Digestion with  $\gamma$ -amylase enzymes is useful for the study of biochemical features of wasteosomes since a 68,4 % of their structure is formed by carbohydrates. It is known  $\alpha$ -amylase and  $\gamma$ -amylase (also known as amyloglucosidase) can digest wasteosomes, as well do  $\beta$ -amylase and phosphorylase in a minor degree. However, it must be reminded that the aggregated structure of wasteosomes can reduce the ability of the enzymes to digest them (3). These enzymes break  $\alpha$ -glycosidic linkages of polymerised hexoses, although each one has specific characteristics. Features for  $\gamma$ -amylase are detailed in [Table 2](#) for (3,33). Extra information about the other amylolytic enzymes can be found in [Annex 3](#).

*Table 2: Features of  $\gamma$ -amylase concerning the glycosidic linkages broken by its action, its breaking mode, the products released and its action blockers.*

Enzyme	Glycosidic linkage broken	Breaking mode	Product	Action blocked by
$\gamma$ -amylase (amyloglucosidase)	$\alpha$ -1:4 and $\alpha$ -1:6 at the outside end of the polyglucosan	from the non-reducing end of the chain	Glc	two or more $\alpha$ -1:6 linkages in one chain, Glc-6-phosphate

Haematoxylin staining is used to visualise cell nuclei, as the haematoxylin solution is a basic dye that stains nucleic acids in deep blue-purple colour (34).

Hoechst staining is also used to visualise cell nuclei, as this fluorescent stain binds to regions of DNA rich in adenine and thymine of the minor groove, emitting a blue light when excited with UV light at 355 nm (35).

### 3.3. METHODS

#### 3.3.1. Lugol's iodine staining

Frozen hippocampal sections were left defrosting for 10 min at room temperature (RT) and then, a drop of Lugol's iodine was added. Lugol's iodine was prepared with 10% KI (793582-100G, Sigma-Aldrich) and 5% iodine (326143-10G, Sigma-Aldrich) in distilled water (H<sub>2</sub>O<sub>d</sub>).

Finally, sections were coverslipped and kept in refrigeration to prevent rotting.

#### 3.3.2. PAS staining

Frozen hippocampal sections were left to defrost and airdry for 10 min at RT. Next, they were fixed with Carnoy's solution (60 % ethanol - ET00061000, Scharlau; 30 % chloroform -131252, Panreac; and 10 % glacial acetic acid - AC03431000, Scharlau) for 10 min, and washed in H<sub>2</sub>O<sub>d</sub> 10 times by immersion. Sections were then pre-treated with 0,25 % periodic acid (19324-50, Electron Microscopy Sciences) in H<sub>2</sub>O<sub>d</sub> for 10 min, and washed in H<sub>2</sub>O<sub>d</sub> for 3 min. After, sections were treated with Schiff's reagent<sup>3</sup> (26052-06, Electron Microscopy Sciences) for 10 min, and washed in H<sub>2</sub>O<sub>d</sub> for about 5 min, until they turned slightly pink. Then, nuclei from sections were counterstained with haematoxylin (3870, J.T. Baker) for 1 min.

Finally, sections were washed 3 times in H<sub>2</sub>O<sub>d</sub>, first by immersion, then for 30 sec and lastly for 1 min. The washes were followed by dehydration with a progression of alcohols and xylene<sup>4</sup> (XI00502500, Scharlau). The dehydration procedure started with immersion in alcohol 70 °, continued with immersion in alcohol 90 °, then immersion in alcohol 100 ° twice for 5 min each, and finally, immersion in xylene twice for 10 min each. The different alcohols used were prepared with ethanol absolute (ET00051000, Scharlau) and H<sub>2</sub>O<sub>d</sub>. Sections were then coverslipped with Eukitt (Eukitt, Fluka Analytical) and a drop of xylene, and then kept at RT.

---

<sup>3</sup> Light protection and refrigeration needed. Cytotoxic.

<sup>4</sup> Fume extractor hood needed.

### 3.3.3. ConA staining

Frozen hippocampal sections were left to defrost and airdry for 10 min at RT. Next, they were rehydrated in phosphate-buffered saline (PBS) for 5 min, and then blocked and permeabilised with blocking buffer (BB) with 0,1% Triton X-100 (BB-T; T8532-100ML, Sigma-Aldrich) for 20 min, at RT, inside a humidified chamber. BB was prepared with 1% bovine serum albumin (A3059-50G, Sigma-Aldrich) in PBS. Following, sections were washed in PBS twice for 5 min each and incubated overnight with fluorescein-labelled ConA<sup>5</sup> (ConA-Fl; 1:250 in PBS; FL-1001-25, Vector Laboratories) at 4 °C, inside a humidified chamber.

After incubation with ConA-Fl, nuclei from sections were stained with Hoechst<sup>6</sup> (2mg/mL; H-33258, Fluka) for 5 min, at RT, inside a humidified chamber.

Finally, sections were washed in PBS twice for 5 min each, and coverslipped with Fluoromount (17984-25, Electron Microscopy Sciences). Slides were left at RT with desiccant balls for 2-3 h and then kept in refrigeration to prevent rotting.

### 3.3.4. Double indirect immunofluorescence (hIgM and $\alpha$ -p62)

Frozen hippocampal sections were left to defrost and airdry for 10 min at RT. Next, they were rehydrated in PBS for 5 min, and then blocked and permeabilised with BB-T for 20 min, at RT, inside a humidified chamber. Then, sections were washed in PBS twice for 5 min each and incubated overnight with the primary Ab<sub>s</sub> at 4 °C, inside a humidified chamber. Next, sections were washed in PBS twice for 5 min each, and incubated with the secondary Ab<sub>s</sub> for 55 min, at RT, inside a humidified chamber.

The primary Ab<sub>s</sub> used in the immunofluorescences were: purified hIgM (1:25 in BB; I8260, Sigma) and mouse monoclonal IgG<sub>2a</sub>  $\alpha$ -p62 (1:250 in BB, ab56416, Abcam). The corresponding secondary Ab<sub>s</sub> used were: goat Ab against hIgM ( $\mu$  chain specific) labelled to Alexa Fluor (AF) 488<sup>7</sup> (1:250 in BB; A-21215, Life Technologies) and goat Ab against mouse IgG<sub>2a</sub> labelled to AF555<sup>8</sup> (1:250 in BB; A-21131, Life Technologies).

After incubation with the secondary Ab<sub>s</sub>, nuclei from sections were stained with Hoechst<sup>9</sup> (2mg/mL) for 5 min, at RT, inside a humidified chamber.

---

<sup>5</sup> Light protection needed.

<sup>6</sup> Light protection needed. Cytotoxic.

<sup>7</sup> Light protection needed.

<sup>8</sup> Light protection needed.

<sup>9</sup> Light protection needed. Cytotoxic.

Finally, sections were washed in PBS twice for 5 min each, and coverslipped with Fluoromount. Slides were left at RT with desiccant balls for 2-3 h and then kept in refrigeration to prevent rotting.

### 3.3.5. Digestion with $\gamma$ -amylase

According to Sakai *et al.* conditions, 10 U/mL of  $\gamma$ -amylase in buffer acetate (BA; 0,016 M in H<sub>2</sub>Od, pH 4,8) at 45 °C, during 8 h, is enough to digest wasteosomes in hippocampal sections (3,33).

Preliminary digestion studies were conducted to determine the exact conditions for the digestion of wasteosomes. Different concentrations (10, 50, 100 and 200 U/mL) and times (22, 8 and 4 h) were tried until finding the suitable requirements. The final conditions selected to conduct our digestion studies were 100 and 200 U/mL of  $\gamma$ -amylase, during 22 h, at 45 °C.

First, PBS was left outside the fridge and  $\gamma$ -amylase outside the freezer to temper their temperature. At the same time, the heater and a water bath prepared with H<sub>2</sub>Od were turned on at 45 °C. The  $\gamma$ -amylase solutions, 100 and 200 U/mL (saturation concentration), were prepared from a lot of 40 U/mg of  $\gamma$ -amylase ( $\alpha$ -amylase from porcine pancreas, type VI-B,  $\geq 5$  units / mg solid; A3176-500KU, Sigma-Aldrich) in cold BA (0,016 M H<sub>2</sub>Od, pH 4,8). Cold temperature for BA was used to enhance  $\gamma$ -amylase solubilization.

Next, frozen hippocampal sections were left to defrost and airdry for 10 min at RT. Meanwhile, the enzyme solutions and the BA were left in the water bath to pre-heat for the selected digestion conditions. Sections were rehydrated in PBS for 5 min, and then covered with 200  $\mu$ L of the pertinent pre-heated solution: BA for the control slides and 100 or 200 U/mL for the other slides. Slides were left in the heater for 22 h, at 45 °C, inside a humidified chamber and in a humidified environment<sup>10</sup> to prevent desiccation.

After the digestions, all slides were washed in PBS 3 times for 5 min each, and then treated (except for the first step of defrost and airdry) as described above for Lugol's iodine staining, ConA staining, PAS staining and double indirect immunofluorescence with hIgM and  $\alpha$ -p62.

### 3.3.6. Image acquisition and processing

Images were obtained using a fluorescence laser and optical microscope (BX41, Olympus, Germany) with the *CellB* software (Olympus) and stored in *tiff* format. For

---

<sup>10</sup> Small water reservoirs were put inside the heater.

Lugol's iodine and PAS staining, images were captured with the bright field mode. For ConA staining and the immunofluorescence detection of the NE and the p62, images were captured with the fluorescence mode.

All images were taken using the same microscope, light adjust or laser, and *CellB* settings. Only time exposure was modified depending on the staining and microscope magnification, but it was kept in the same conditions for the treated samples and their respective controls corresponding to the same staining. After, images were adjusted using the *ImageJ* program (National Institute of Health, USA). Colour balance was modified depending on the staining, to make it out, and the corresponding controls were treated the same way. Merging of the images of ConA staining and the immunofluorescence detection of the NE and the p62 with their respective images stained with Hoechst was also performed using the *ImageJ* program.

## 4. RESULTS AND DISCUSSION

### 4.1. CHARACTERISATION OF THE HIPPOCAMPAL SECTIONS

To facilitate the exposition and discussion of the results, the hippocampal sections have been analysed focusing on three different areas. These selected zones are: the hippocampal sulcus, the fimbriodentate sulcus, and the dentate gyrus.

Firstly, an image of the human brain and the human hippocampus are shown in Fig. 5 to help the reader localise the previously commented areas, as well as some others which may be of help.

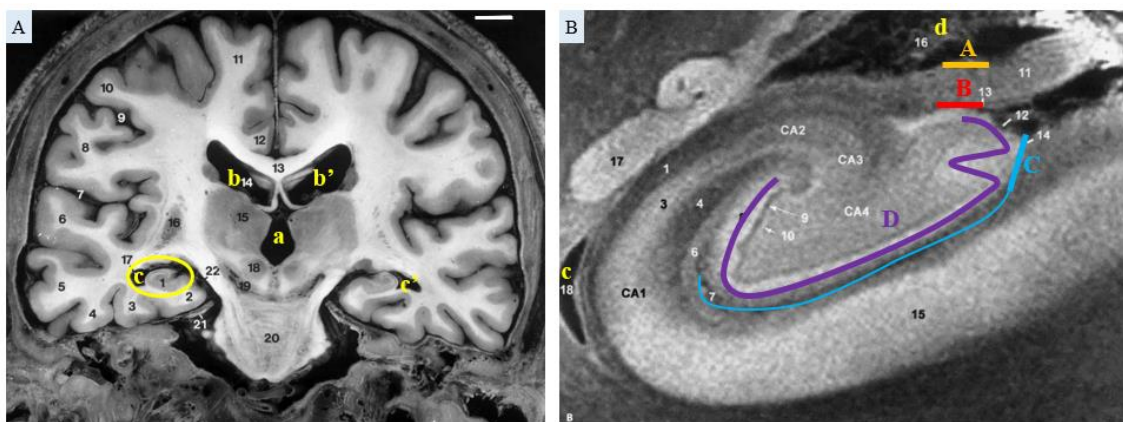


*Figure 5: Coronal section of the human brain (A) and view of the structure of the hippocampus (B) obtained by magnetic resonance imaging. Scale bar: 10 mm (A) and unknown (B). For image A: a, third ventricle; b and b', lateral ventricles (with their temporal horn indicated as c and c'); left hippocampus is encircled. For image B: c, temporal horn of the lateral ventricle; d, choroid plexus; A, choroidal fissure; B, fimbriodentate sulcus; C, hippocampal sulcus; D, dentate gyrus. Adapted from (36).*

As mentioned in the introduction, wasteosomes are concentrated in perivascular, periventricular and subpial regions, which can be related to the extrusion of these bodies from the brain parenchyma to the CSF. This is the reason why we decided to focus our study and analysis of the results especially on the areas with a higher number of wasteosomes, which are mainly the bordering areas of the hippocampus. As can be seen in Fig. 5, within these bordering areas, the hippocampal sulcus and the fimbriodentate sulcus are more peripheral areas, whereas the dentate gyrus is a more inner area.

To continue with the localisation of the selected areas for our study, images of the three cases are shown in Fig. 6-8. These areas were chosen due to the higher presence of wasteosomes in them.

### Hippocampal section of case 1

The studied areas for case 1 can be seen in Fig. 6. These areas were: the hippocampal and the fimbriodentate sulcus in the peripheral zones, and the dentate gyrus in the inner zone.

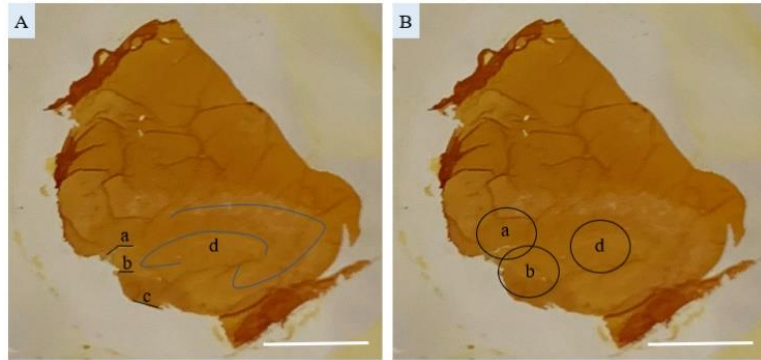


*Figure 6: Hippocampal section of case 1 stained with Lugol's iodine. Areas from which images were taken when using the microscope are shown in B. For A and B: a, hippocampal sulcus; b, fimbriodentate sulcus; c, choroidal fissure; d, dentate gyrus. Scale bar: 0,65 cm.*

### Hippocampal section of case 2

The studied areas for case 2 can be seen in Fig. 7. These areas were: the hippocampal and the fimbriodentate sulcus, both of which are in a peripheral zone.

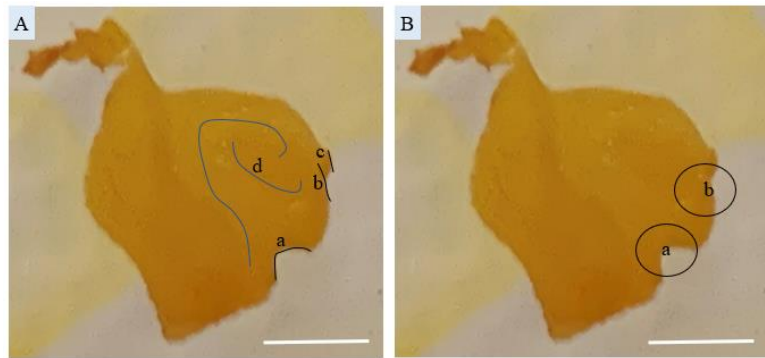


*Figure 7: Hippocampal section of case 2 stained with Lugol's iodine. Areas from which images were taken when using the microscope are shown in B. For A and B: a, hippocampal sulcus; b, fimbriodentate sulcus; c, choroidal fissure; d, dentate gyrus. Scale bar: 0,65 cm.*

### Hippocampal section of case 3

The studied areas for case 3 can be seen in Fig. 8. These areas were: the beginning of the hippocampal sulcus and the ending of it, both of which can be considered peripheral zones.



*Figure 8: Hippocampal section of case 3 stained with Lugol's iodine. Areas from which images were taken when using the microscope are shown in B. For A and B: a, hippocampal sulcus; b, fimbriodentate sulcus; c, choroidal fissure; d, dentate gyrus. Black arrow: rests of embedding medium. Scale bar: 0,65 cm.*

## 4.2. PRELIMINARY STUDIES

The preliminary staining studies were conducted with case 1 and results, shown in Fig. 9, allowed to validate Lugol's iodine staining, PAS staining, ConA staining and the immunofluorescence detection of the NE and the p62 as good techniques for the detection of wasteosomes in hippocampal sections. As expected, Lugol's iodine stained wasteosomes in brown (a), whereas PAS stained them in pink (b). As regards to the fluorescent stainings, ConA stained wasteosomes in a homogenous and noticeable green (c), whereas  $\mu$ IgM stained them in a not so homogeneous nor intense green (d<sub>1</sub> and d<sub>3</sub>), and, to finish,  $\alpha$ -p62 staining resulted in an intense red concentrated in the peripheral area of some of these structures (d<sub>2</sub> and d<sub>3</sub>).

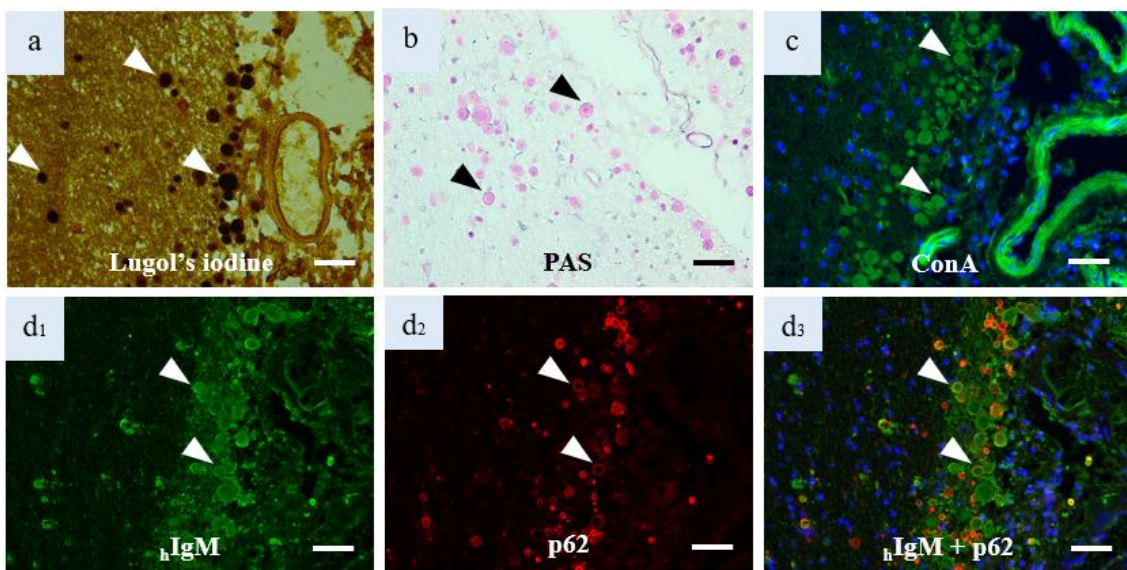


*Figure 9: Preliminary staining studies of case 1. a, Lugol's iodine (brown); b, PAS (pink); c, merging ConA + Hoechst (green + blue); d<sub>1</sub>,  $\mu$ IgM, (green); d<sub>2</sub>,  $\alpha$ -p62 (red); d<sub>3</sub>, merging  $\mu$ IgM +  $\alpha$ -p62 + Hoechst (green + red + blue). Black and white arrowheads: wasteosomes. Images taken at 200x - Scale bar: 50  $\mu$ m.*

In relation to the preliminary studies with  $\gamma$ -amylase, as can be seen in Fig. 10, the selected conditions were appropriate for the digestion of wasteosomes. With small microscope magnification, a reduction in the intensity of Lugol's iodine staining was noticed from 0 (a<sub>1</sub>) to 200 U/mL (c<sub>1</sub>) of  $\gamma$ -amylase, as well as a reduction in the number of wasteosomes, which can be seen as small brown spots. With higher magnification, at 100 (b<sub>2</sub>) and especially at 200 U/mL (c<sub>2</sub>) of  $\gamma$ -amylase, empty spots were seen in the places where wasteosomes had been completely digested.

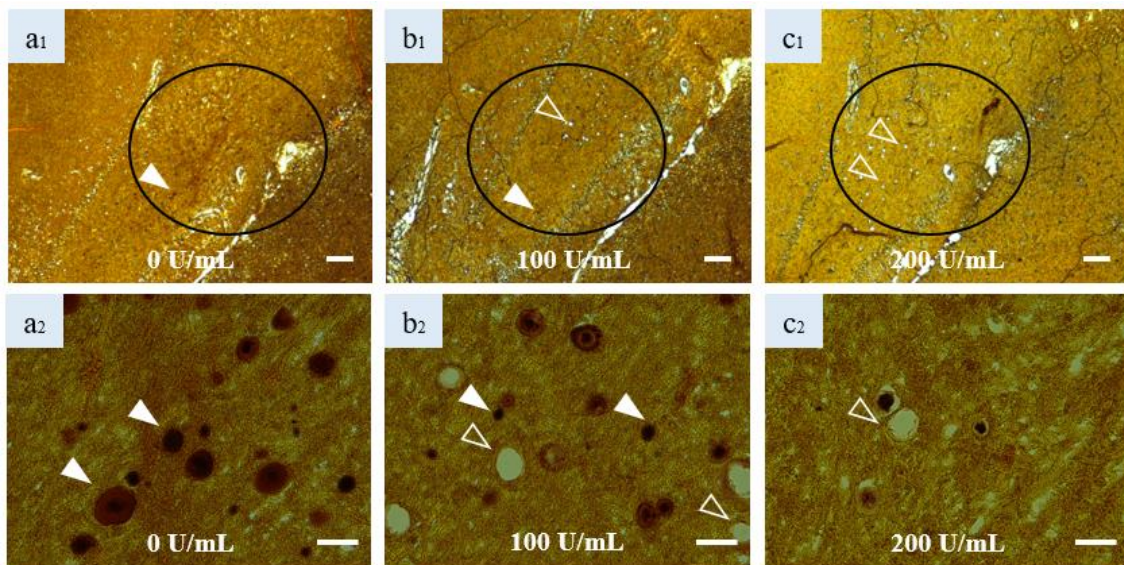


**Figure 10:** Preliminary digestion studies of case 1 conducted with two different concentrations of  $\gamma$ -amylase and followed by Lugol's iodine (brown) staining. **a**, control samples treated with 0 U/mL, at 45 °C, for 22 h; **b**, samples treated with 100 U/mL, at 45 °C, for 22 h; **c**, samples treated with 200 U/mL of  $\gamma$ -amylase, at 45 °C, for 22 h. **a<sub>2</sub>**, **b<sub>2</sub>** and **c<sub>2</sub>** correspond to the encircled areas in **a<sub>1</sub>**, **b<sub>1</sub>** and **c<sub>1</sub>**. White arrowheads: wasteosomes; white arrowhead outlines: empty spots left by digested wasteosomes. Images with subindex 1 taken at 40x - Scale bar: 100  $\mu$ m. Images with subindex 2 taken at 400x - Scale bar: 50  $\mu$ m.

### 4.3. DIGESTION STUDIES WITH $\Gamma$ -AMYLASE

#### 4.3.1. Effect of $\gamma$ -amylase on Lugol's iodine staining of wasteosomes

As can be noticed in Fig. 11, from cases 1 (*a-c*) and 2 (*d* and *e*), Lugol's iodine staining and the effects of digestion with  $\gamma$ -amylase changed depending on the location of wasteosomes in the hippocampus, suggesting there may exist some differences between these polyglucosan structures.

Apparently, wasteosomes located in the proximities of the dentate gyrus, which is a more inner area, tended to disappear after treatment with 100 U/mL (*b<sub>2</sub>*) and more distinctly after treatment with 200 U/mL (*b<sub>3</sub>*) of  $\gamma$ -amylase. The disappearance could even be seen, in some cases, as a hole in the tissue where the wasteosomes used to be (*b<sub>3</sub>*). On the contrary, wasteosomes located in more peripheral areas such as the immediacies of the hippocampal sulcus and the fimbriodentate sulcus (*a*, *c-e*), remained almost intact or only showed a minor decrease in their staining. The reduction in the staining started in the outlines of the structures, as shown in the insets of images *b<sub>2</sub>* and *b<sub>3</sub>* (*b<sub>2,2</sub>* and *b<sub>3,2</sub>*), in which wasteosomes can be seen stained in lighter brown in the peripheral areas, stained in the centre and leaving an empty spot in the peripheral areas, or leaving only an empty spot.

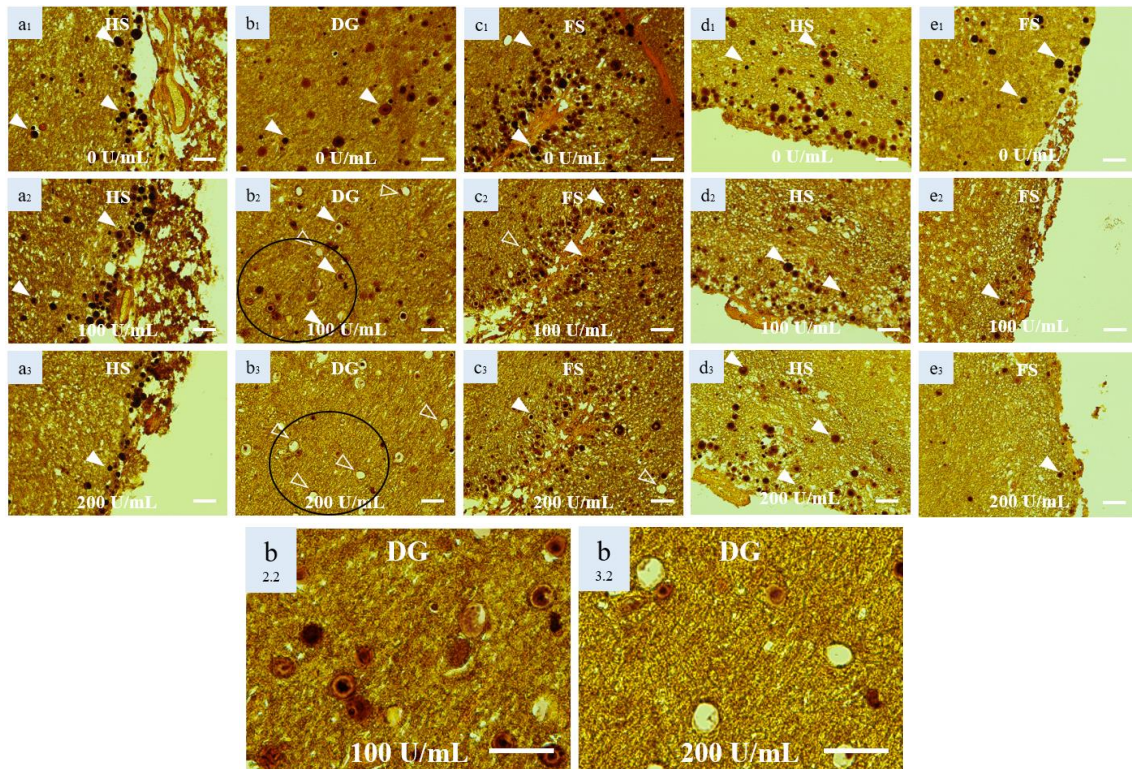


**Figure 11:** Lugol's iodine (brown) staining of cases 1 (a-c) and 2 (d and e) after digestion with  $\gamma$ -amylase at 0 U/mL (control samples; images with subindex 1), 100 U/mL (images with subindex 2) and 200 U/mL (images with subindex 3) for 22 h, at 45 °C. Differences can be seen between wasteosomes located in inner and wasteosomes located in peripheral areas of the hippocampal sections. Insets of images b<sub>2</sub> and b<sub>3</sub> have been added to help the visualisation (b<sub>2.2</sub> and b<sub>3.2</sub>). White arrowheads: wasteosomes; white arrowhead outlines: empty spots left by digested wasteosomes. HS, hippocampal sulcus; DG, dentate gyrus; FS, fimbriodentate sulcus. Images taken at 200x - scale bar: 50  $\mu$ m.

#### 4.3.2. Effect of $\gamma$ -amylase on PAS staining of wasteosomes

Although results from PAS staining after digestion were not as clear as the ones obtained with Lugol's iodine, Fig. 12 shows how in case 3 there was a reduction in the number of wasteosomes stained after digestion with  $\gamma$ -amylase. Such reduction in number was more obvious in pictures taken at less magnification (b), which belong to consecutive hippocampal sections, one of them from a control sample (b<sub>1</sub>). Nevertheless, an intensity measurement should be conducted to give a more accurate explanation of the effect of  $\gamma$ -amylase.

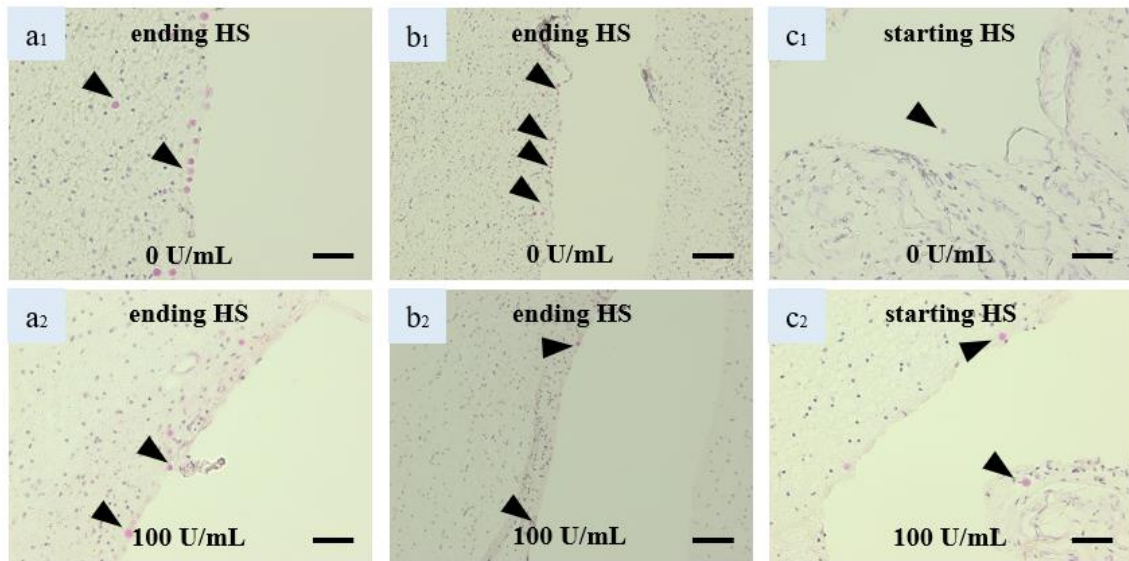


**Figure 12:** PAS (pink) staining of the hippocampal section of case 3 after digestion with  $\gamma$ -amylose at 0 U/mL (control samples; images with subindex 1) and 100 U/mL (images with subindex 2) for 22 h, at 45 °C. A reduction in the number of wasteosomes can slightly be appreciated when comparing control samples and treated samples. Black arrowheads: wasteosomes. HS, hippocampal sulcus. Images **a** and **c** taken at 200x – scale bar: 50  $\mu$ m; images **b** taken at 100x – scale bar: 100  $\mu$ m.

Moreover, it could be added that the number of wasteosomes stained, whether there was or not a digestion treatment, was major in the area matching the ending part of the hippocampal sulcus. However, no difference in the staining has been noticed between this region and the beginning part of the hippocampal sulcus.

#### 4.3.3. Effect of $\gamma$ -amylose on ConA staining of wasteosomes

As can be noticed in Fig. 13, from cases 1 (*a* and *b*) and 2 (*c* and *d*), ConA staining and the effects of digestion with  $\gamma$ -amylose varied depending on the location of wasteosomes in the hippocampus, suggesting again there may exist some differences between these polyglucosan structures.

Seemingly, wasteosomes located in the proximities of the dentate gyrus, which is a more inner area, did not even stain with ConA in the non-digested sample (*b*<sub>1</sub>). The lack of stain was very perceptible when comparing image *b*<sub>1</sub> with images *a*<sub>1</sub>, *c*<sub>1</sub> and *d*<sub>1</sub>. On the contrary, wasteosomes located in the immediacies of the hippocampal sulcus and the fimbriodentate sulcus (*a*, *c*-*d*), which are more peripheral areas, experimented a noticeable decrease of their staining after being treated with 100 U/mL (*a*<sub>2</sub>, *c*<sub>2</sub> and *d*<sub>2</sub>) and completely lost their staining after treatment with 200 U/mL of  $\gamma$ -amylose (*a*<sub>3</sub>, *b*<sub>3</sub> and *d*<sub>3</sub>).

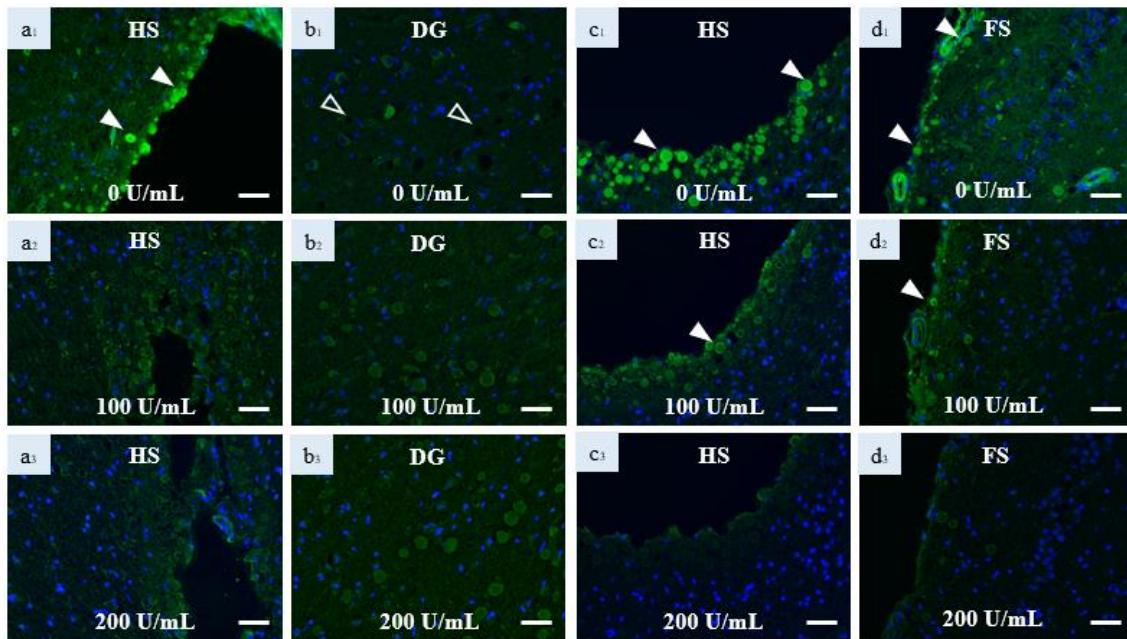


**Figure 13:** ConA (green) and Hoechst (blue) staining of cases 1 (a and b) and 2 (c and d) after digestion with  $\gamma$ -amylase at 0 U/mL (control samples; images with subindex 1), 100 U/mL (images with subindex 2) and 200 U/mL (images with subindex 3) for 22 h, at 45 °C. Differences can be seen between wasteosomes located in inner and wasteosomes located in peripheral areas of the hippocampal section. White arrowheads: wasteosomes; white arrowhead outlines: empty spots left by non-stained wasteosomes. HS, hippocampal sulcus; DG, dentate gyrus; FS, fimbriodentate sulcus. Images taken at 200x - scale bar: 50  $\mu$ m.

#### 4.3.4. Effect of $\gamma$ -amylase on double indirect immunofluorescence (with $^h$ IgM and $\alpha$ -p62) of wasteosomes

Regarding the staining of the NE from cases 1 (a and b) and 2 (c and d), shown in Fig.14, all wasteosomes from control samples were labelled with  $^h$ IgM, although in the area corresponding to the dentate gyrus ( $b_1$ ), the staining was less intense. After treatment with  $\gamma$ -amylase, there was a noticeable loss of the staining in the inner area of the hippocampal section, the dentate gyrus ( $b_2$  and  $b_3$ ). Contrary, the immediacies of the hippocampal sulcus and the fimbriodentate sulcus (a, c-d) seemed to experiment a smaller decrease in the staining ( $a_2$  and  $a_3$ ) or even a very slightly decrease ( $c_2$ ,  $c_3$ ,  $d_2$  and  $d_3$ ).

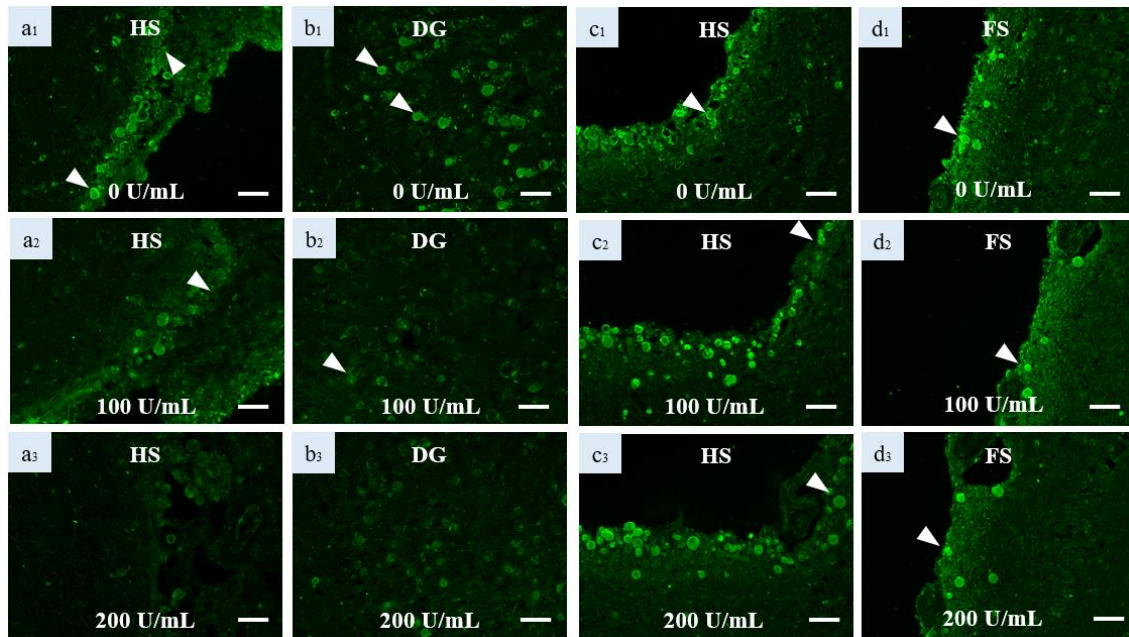


**Figure 14:** Indirect immunofluorescence with  $\mu$ IgM (green) of cases 1 (a and b) and 2 (c and d) after digestion with  $\gamma$ -amylase at 0 (control samples; images with subindex 1), 100 U/mL (images with subindex 2) and 200 U/mL (images with subindex 3) for 22 h, at 45 °C. Differences can be seen between wasteosomes located in inner and wasteosomes located in peripheral areas of the hippocampal section. White arrowheads: wasteosomes. HS, hippocampal sulcus; DG, dentate gyrus; FS: fimbriodentate sulcus. Images taken at 200x - scale bar: 50  $\mu$ m.

Regarding the staining of the p62 from cases 1 (a and b) and 2 (c and d), shown in Fig.15, the pattern was different from the one observed for the NE. In this case, all wasteosomes from control samples were labelled with  $\alpha$ -p62, although in the area corresponding to the dentate gyrus ( $b_1$ ), the staining showed a higher intensity in comparison to more peripheral areas such as the immediacies of the hippocampal sulcus and the fimbriodentate sulcus ( $a_1$ ,  $c_1$ - $d_1$ ). After treatment with  $\gamma$ -amylase and regardless of the localization of wasteosomes, in all cases there was a noticeable decrease of the staining of p62. Nevertheless, it can be pointed out that the decrease in the hippocampal sulcus in  $c_2$  and  $c_3$  was not as intense as expected. Nevertheless, intensity should be quantified to give a better assessment.

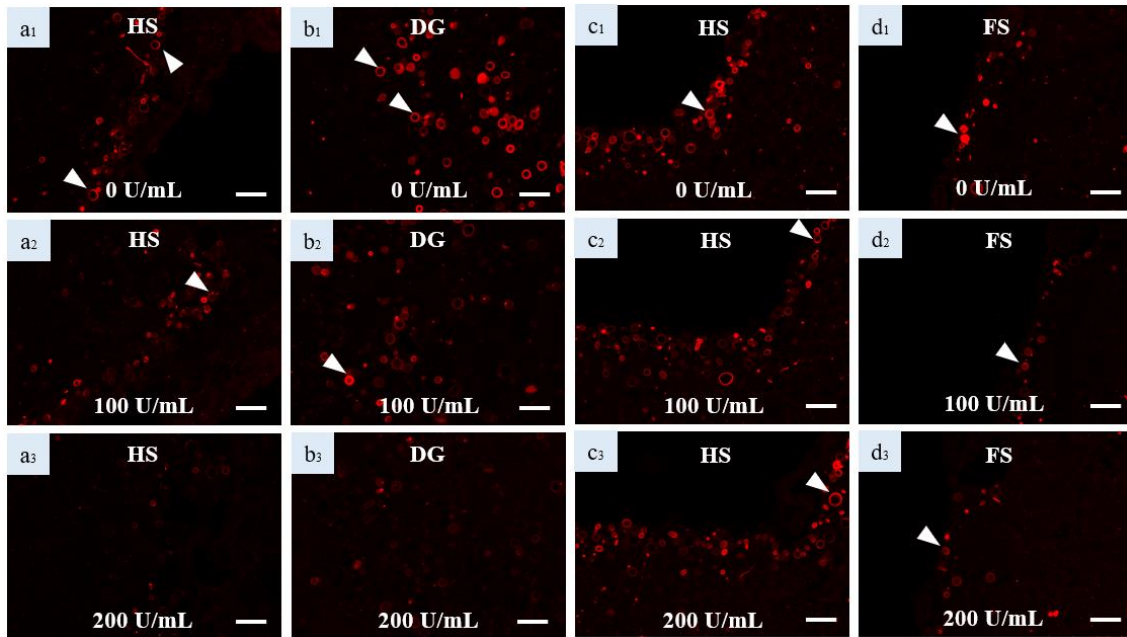


**Figure 15:** Indirect immunofluorescence with  $\alpha$ -p62 (red) of cases 1 (a and b) and 2 (c and d) after digestion with  $\gamma$ -amylase at 0 (control samples; images with subindex 1), 100 U/mL (images with subindex 2) and 200 U/mL (images with subindex 3) for 22 h, at 45 °C. Differences can be seen between wasteosomes located in inner and wasteosomes located in peripheral areas of the hippocampal section. White arrowheads: wasteosomes. HS, hippocampal sulcus; DG, dentate gyrus; FS, fimbriodentate sulcus. Images taken at 200x - scale bar: 50  $\mu$ m.

Finally, the merging of the images from the immunofluorescence with  $hIgM$  and  $\alpha$ -p62 (Fig.14 and 15) from cases 1 (a and b) and 2 (c and d) are shown in Fig.16. As it has already been noticed, the double indirect immunofluorescence with  $hIgM$  and  $\alpha$ -p62 and the effects of digestion with  $\gamma$ -amylase varied depending on the location of wasteosomes in the hippocampus, suggesting once more there may exist some differences between these polyglucosan structures. It can be summarised that wasteosomes in inner areas of the hippocampal sections were significantly stained with  $\alpha$ -p62 but not with  $hIgM$ , whereas those in more peripheral areas exposed a strong  $hIgM$  staining but a weak p62 staining. Finally, it must be mentioned that the merging of the results from  $hIgM$  and p62 staining showed that not all of the wasteosomes were stained with p62.

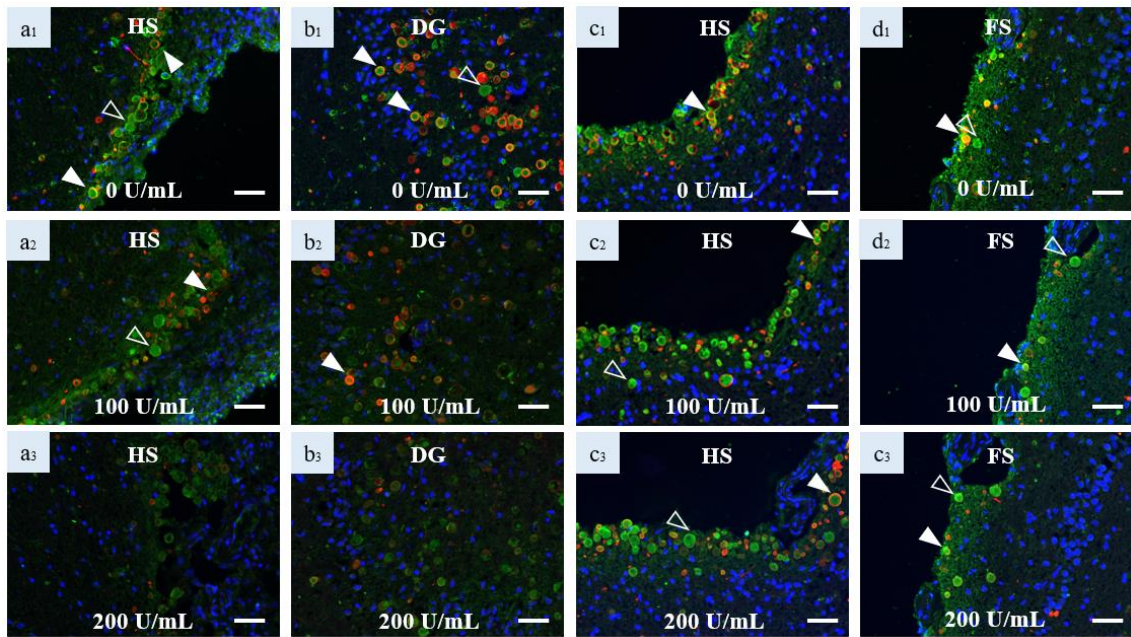


**Figure 16:** Double indirect immunofluorescence with  $hIgM$  (green) and  $\alpha$ -p62 (red) and Hoechst (blue) staining of cases 1 (a and b) and 2 (c and d) after digestion with  $\gamma$ -amylase at 0 U/mL (control samples; images with subindex 1), 100 U/mL (images with subindex 2) and 200 U/mL (images with subindex 3) for 22 h, at 45 °C. Differences can be seen between wasteosomes located in inner and wasteosomes located in peripheral areas of the hippocampal section. White arrowheads: wasteosomes; white arrowhead outlines: wasteosomes stained with  $hIgM$  but not with p62. HS, hippocampal sulcus; DG, dentate gyrus; FS, fimbriodentate sulcus. Images taken at 200x - scale bar: 50  $\mu$ m.

Finally, to summarise the behaviour of wasteosomes when stained, with or without previous digestion, results have been summarised in a schematic way in [Table 3](#).

**Table 3:** Summarised results of the staining of wasteosomes, with ( $\gamma$ -amylase) or without ( $\gamma$ -amylase) previous digestion with  $\gamma$ -amylase. IN: wasteosomes in inner areas; PER: wasteosomes in peripheral areas. Staining of wasteosomes with **Lugol's iodine**: ●, stained; ○, only peripheral staining; ○, no staining. Staining of wasteosomes with **PAS**: ●, stained. Staining of wasteosomes with **ConA**: ●, stained; ○, only peripheral staining; ○, no staining. Staining of wasteosomes with  $hIgM$ : ●, stained; ○, only peripheral staining; ○, no staining. Staining of wasteosomes with  $\alpha$ -p62: ○, stained; ○, no staining.

	Lugol's iodine		PAS		ConA		$hIgM$ and $\alpha$ -p62	
	IN	PER	IN	PER	IN	PER	IN	PER
$\gamma$ -amylase		●		●	○	●	●	○
$\gamma$ -amylase	○	● ○	not studied	● reduction in number	○	○ ○	○ ○	○ ○ ○

#### 4.4. INTEGRATION OF THE RESULTS

As an overview, wasteosomes are spherical polyglucosan bodies that amass waste substances. They are generated in the CNS during normal aging and neurodegenerative processes, then extruded into the CSF and finally, they reach the cervical lymph nodes, where they are phagocytised by macrophages. These polyglucosan structures contain p62 and NE of carbohydrate nature that can be detected by  $^h$ IgM. All in all, it is likely to think wasteosomes are implicated in the cleaning of brain waste substances.

In this work, the staining techniques combined with digestion with  $\gamma$ -amylase have shown that wasteosomes present different features according to their location in the human hippocampus.

First, Lugol's iodine staining, which allows the visualisation of glycan polymers such as starch and glycogen, reaffirmed wasteosomes are undoubtedly polyglucosan bodies, as the staining was, to a greater or lesser extent, affected by the treatment with  $\gamma$ -amylase. In fact, results before and after treatment with the enzyme varied depending on the location of these bodies. Such different behaviour suggests there are different types of wasteosomes regarding their glycan composition. It can be mentioned wasteosomes in peripheral areas have a more resistant polyglucosan structure towards digestion than wasteosomes in more inner areas, since the staining of the first ones barely decreased after treatment with  $\gamma$ -amylase. This proposal suggests that wasteosomes in inner areas have a polyglucosan structure more branched and less phosphorylated, whereas that of wasteosomes in peripheral is less branched and mainly phosphorylated. Such deductions are supported by amylose staining with Lugol's iodine in deep blue-black and amylopectin in reddish-purple. Furthermore, the fact that phosphorylation reduces the capacity of  $\gamma$ -amylase to break glycosidic linkages and that branched structures are less compacted and more accessible for the enzyme, help validate these deductions.

Following with PAS staining, this technique also demonstrated wasteosomes are polyglucosan bodies, given that it exhibits carbohydrates and that our bodies were stained. In this case, results showed a noticeable decrease in the number of wasteosomes stained after digestion with  $\gamma$ -amylase, although it must be said it was a qualitative deduction.

Next, and besides exhibiting again wasteosomes are polyglucosan bodies, ConA staining added some information to the deductions obtained from Lugol's iodine staining. Results showed no detection of wasteosomes in inner areas when no digestion was applied and a noticeable reduction in the staining in peripheral areas after digestion. These facts could indicate that wasteosomes located in inner areas lack some essential saccharides for the binding of ConA and imply that  $\gamma$ -amylase eliminates some of these saccharides, essential for the binding of ConA, contained in wasteosomes of peripheral areas.

Regarding the staining of the NE, since it was softer and decreased notably in wasteosomes located in inner areas after digestion with  $\gamma$ -amylase, it appears that wasteosomes in peripheral areas have greater amounts of NE and, again, a more resistant polyglucosan structure towards digestion. On the contrary, for p62 the pattern was different. The staining was more intense in inner areas in comparison to more peripheral areas and, after treatment with  $\gamma$ -amylase and regardless of the localization of wasteosomes, in all cases it experimented a noticeable decrease. Such reduction could be explained by considering that p62 is bound or entrapped in the polyglucosan structure of wasteosomes, and therefore liberated after digestion with  $\gamma$ -amylase. As a result, it could be stated that wasteosomes located in inner areas of the hippocampal section contain less NE and more p62, while wasteosomes in peripheral areas contain more NE and less p62. In addition, the merging of our immunofluorescence results revealed that not all wasteosomes contain p62, something unexpected as we had not described it in our previous studies (10). However, this finding can be explained since not all brain waste substances, such as membranous vesicles, need p62 labelling to be processed, and therefore, some wasteosomes may not contain any waste substance labelled to p62.

Taken together, results exhibit, at least, two subtypes of wasteosomes in the human hippocampus. Concretely, wasteosomes located in inner areas of the hippocampus contain higher amounts of p62, exhibit lower amounts of NE, and are easily digested with  $\gamma$ -amylase. Conversely, wasteosomes located in peripheral areas of the hippocampus contain lower amounts of p62, higher amounts of NE, and have a more resistant polyglucosan structure towards digestion. For these reasons, it could be proposed that inner wasteosomes may present a less phosphorylated and a more branched amylopectin-like polymer easily attacked with  $\gamma$ -amylase, whereas peripheral wasteosomes might present a mainly phosphorylated and a less branched amylose-like polymer structure that makes them resistant to the effect of  $\gamma$ -amylase. Nevertheless, it is needed to continue the study with a higher number of samples and quantify all results for a later statistical analysis.

Considering that wasteosomes undergo a process from an immature to a mature state, it is conceivable that the differences between these bodies in our study are due to this process. In this sense, wasteosomes in the inner areas would be immature, whereas wasteosomes in the peripheral areas would be more mature. We propose that in their preliminary stages, wasteosomes would accumulate waste substances inside, which would explain their higher amount of p62 when located in inner areas of the hippocampal sections. Then, the polyglucosan structure of the body would be developed to entrap waste substances and together with the higher concentration of these substances, the NE would be formed. This would explain why wasteosomes located in more peripheral areas express more NE and are more resistant to the action of the  $\gamma$ -amylase. These mature wasteosomes in peripheral areas would be ready to be extruded from brain parenchyma

to the CSF and finally eliminated via a phagocytosis process, which still needs more study, in the cervical lymph nodes.

As concerns to the enzyme digestions conducted by Sakai *et al.* (3), our study provides with the observation of two subtypes of wasteosomes. Sakai *et al.* worked with tissue sections but focused on the study of isolated wasteosomes. In the study of tissue sections, they did not find differences between wasteosomes since all wasteosomes were digested with  $\gamma$ -amylase. In the study of isolated wasteosomes, encountering differences between wasteosomes based on their location in the brain was not possible. In addition, the treatments applied to isolate the wasteosomes from brain tissue probably disrupted some features of these bodies. Therefore, amplifying the work of Sakai *et al.* and focusing on the study of wasteosomes in hippocampal sections has allowed us to find out that not all wasteosomes are alike.

Finally, the limitations of this work must be mentioned. On the one hand, it should be verified if peripheral wasteosomes correspond to developed wasteosomes in inner areas of the hippocampus. Despite the presence of matrix-metalloproteinase-2 inside these bodies and other mechanisms, maybe still to be discovered, it is not clear that the extracellular remodelling could allow such displacement. On the other hand, and as already mentioned, the reader should consider this is an initial study which needs to be amplified with a higher number of samples from donors of both genders. It could also be interesting to include samples from donors of different races. There are many variables regarding wasteosomes which can affect the results, such as the type of disease and the age of the patient, the post-mortem delay before fixation of the sections..., which added to the regulations regarding studies with human samples, made it very difficult to use more than three donors in our work. It would also be interesting to quantify the results of the different stainings for a later statistical analysis, although the qualitative observations can already be taken into consideration. Moreover, the hippocampus shape changes a bit between people and depending on the section, for which reason not all the same areas of the three donors have been possible to study. For all these reasons, our will is to continue with this study and amplify it.

## 5. CONCLUSIONS

1. There are **two subtypes of wasteosomes** depending on their location in the human hippocampus:
  - a. Wasteosomes in inner areas of the hippocampus contain more p62, less NE and have a less resistant polyglucosan structure towards  $\gamma$ -amylase.
  - b. Wasteosomes in peripheral areas of the hippocampus contain less p62, more NE and have a more resistant polyglucosan structure towards  $\gamma$ -amylase.
2. The differences between these two subtypes could be explained by a **maturation process**:
  - a. Wasteosomes in inner areas are developing immature polyglucosan bodies.
  - b. Wasteosomes in peripheral areas are mature polyglucosan bodies ready to be extruded.
3. The **p62** is **not always present** in wasteosomes.
4. Wasteosomes are involved in a **complex brain waste clearance system** which must be continued to study.

## 6. BIBLIOGRAPHY

1. Virchow R. Ueber eine im gehirn und rückenmark des menschen aufgefundene substanz mit der chemischen reaction der cellulose. *Archiv f pathol Anat.* 1854; 6:135-138. doi: 10.1007/BF01930815
2. Cavanagh JB. Corpora-amylacea and the family of polyglucosan diseases. *Brain Res Rev.* 1999; 29:265-95. doi: 10.1016/S0165-0173(99)00003-X
3. Sakai M, Austin J, Witmer F, Trueb L. Studies of corpora amylacea: isolation and preliminary characterization by chemical and histochemical techniques. *Arch Neurol.* 1969; 21:526-44. doi: 10.1001/archneur.1969.00480170098011
4. Catola G, Achúcarro N. Über die entstehung der amyloidkörperchen im zentralnervensystem. *Virchows Arch Path Anat.* 1906; 184:454-469. doi: 10.1007/BF01999854
5. Pirici D, Margaritescu C. Corpora amylacea in aging brain and age-related brain disorders. *J Aging Gerontol.* 2014; 2:33-57. doi: 10.12974/2309-6128.2014.02.01.6
6. Rohn TT. Corpora amylacea in neurodegenerative diseases: cause or effect? *Int J Neurol Neurother.* 2015; 2:031. doi: 10.23937/2378-3001/2/2/1031
7. Augé E, Cabezón I, Pelegrí C, Vilaplana J. New perspectives on corpora amylacea in the human brain. *Sci Rep.* 2017; 7:41807. doi: 10.1038/srep41807
8. Augé E, Bechmann I, Llor N, Vilaplana J, Krueger M, Pelegrí C. Corpora amylacea in human hippocampal brain tissue are intracellular bodies that exhibit a homogeneous distribution of neo-epitopes. *Sci Rep.* 2019; 9:2063. doi: 10.1038/s41598-018-38010-7
9. Navarro PP, Genoud C, Castaño-Díez D, Graff-Meyer A, Lewis AJ, de Gier Y, et al. Cerebral corpora amylacea are dense membranous labyrinths containing structurally preserved cell organelles. *Sci Rep.* 2018; 8:18046. doi: 10.1038/s41598-018-36223-4
10. Augé E, Duran J, Guinovart JJ, Pelegrí C, Vilaplana J. Exploring the elusive composition of corpora amylacea of human brain. *Sci Rep.* 2018; 8:13525. doi: 10.1038/s41598-018-31766-y
11. Sbarbati A, Carner M, Colletti V, Osculati F. Extrusion of corpora amylacea from the marginal glia at the vestibular root entry zone. *J Neuropathol Exp Neurol.* 1996; 55:196-201. doi: 10.1097/00005072-199602000-0000
12. Riba M, Del Valle J, Augé E, Vilaplana J, Pelegrí C. From corpora amylacea to wasteosomes: history and perspectives. *Ageing Res Rev.* 2021; 72:101484. doi: 10.1016/j.arr.2021.101484
13. Pisa D, Alonso R, Marina AI, Rábano A, Carrasco L. Human and microbial proteins from corpora amylacea of Alzheimer's disease. *Sci Rep.* 2018; 8:9880. doi: 10.1038/s41598-018-28231-1
14. Young LEA, Brizzee CO, Macedo JKA, Murphy RD, Contreras CJ, DePaoli-Roach AA, et al. Accurate and sensitive quantitation of glucose and glucose phosphates derived from storage carbohydrates by mass spectrometry. *Carbohydr Polym.* 2020; 230:115651. doi: 10.1016/j.carbpol.2019.115651
15. Jessen NA, Munk AS, Lundgaard I, Nedergaard M. The glymphatic system: a beginner's guide. *Neurochem Res.* 2015; 40:2583-2599. doi: 10.1007/s11064-015-1581-6
16. Benveniste H, Liu X, Koundal S, Sanggaard S, Lee H, Wardlaw J. The glymphatic system and waste clearance with brain aging: a review. *Gerontology.* 2019; 65:106-119. doi: 10.1159/000490349
17. Riba M, Augé E, Campo-Sabariz J, Moral-Anter D, Molina-Porcel L, Ximelis T, et al. Corpora amylacea act as containers that remove waste products from the brain. *Proc Natl Acad Sci USA.* 2019; 116:26038-26048. doi: 10.1073/pnas.1913741116
18. Tamura R, Yoshida K, Toda M. Current understanding of lymphatic vessels in the central nervous system. *Neurosurg Rev.* 2020; 43:1055-1064. doi: 10.1007/s10143-019-01133-0
19. Kay M. Physiologic autoantibody and immunoglobulin interventions during aging. *Curr Aging Sci.* 2013; 6:56-62. doi: 10.2174/1874609811306010008
20. Vollmers HP, Brändlein S. Natural antibodies and cancer. *N Biotechnol.* 2009; 25:294-8. doi: 10.1016/j.nbt.2009.03.016

- 21.** Grönwall C, Vas J, Silverman GJ. Protective roles of natural IgM antibodies. *Front Immunol.* 2012; 3:66. doi: 10.3389/fimmu.2012.00066
- 22.** Maddur MS, Lacroix-Desmazes S, Dimitrov JD, Kazatchkine MD, Bayry J, Kaveri SV. Natural antibodies: from first-line defense against pathogens to perpetual immune homeostasis. *Clin Rev Allergy Immunol.* 2020; 58:213-228. doi: 10.1007/s12016-019-08746-9
- 23.** Binder CJ. Naturally occurring IgM antibodies to oxidation-specific epitopes. *Adv Exp Med Biol.* 2012; 750:2-13. doi: 10.1007/978-1-4614-3461-0\_1
- 24.** Berland R, Wortis HH. Origins and functions of B-1 cells with notes on the role of CD5. *Annu Rev Immunol.* 2002; 20:253-300. doi: 10.1146/annurev.immunol.20.100301.064833
- 25.** Bovin NV. Natural antibodies to glycans. *Biochemistry (Mosc).* 2013; 78:786-97. doi: 10.1134/S0006297913070109
- 26.** Vollmers HP, Brändlein S. Natural IgM antibodies: the orphaned molecules in immune surveillance. *Adv Drug Deliv Rev.* 2006; 58:755-65. doi: 10.1016/j.addr.2005.08.007
- 27.** Baumgarth N, Tung JW, Herzenberg LA. Inherent specificities in natural antibodies: a key to immune defense against pathogen invasion. *Springer Semin Immunopathol.* 2005; 26:347-62. doi: 10.1007/s00281-004-0182-2
- 28.** Binder CJ. Natural IgM antibodies against oxidation-specific epitopes. *J Clin Immunol.* 2010; 30(suppl 1):S56-60. doi: 10.1007/s10875-010-9396-3
- 29.** Brewer MK, Putaux JL, Rondon A, Uittenbogaard A, Sullivan MA, Gentry MS. Polyglucosan body structure in Lafora disease. *Carbohydr Polym.* 2020; 240:116260. doi: 10.1016/j.carbpol.2020.116260
- 30.** McManus JF. Histological and histochemical uses of periodic acid. *Stain Technol.* 1948; 23:99-108. doi: 10.3109/10520294809106232
- 31.** Varki A, Cummings RD, Esko JD, Stanley P, Hart GW, Aebi M, Darvill AG, Kinoshita T, Packer NH, Prestegard JH, Schnaar RL, Seeberger PH, editors. *Essentials of Glycobiology.* 3rd ed. Cold Spring Harbor (NY): Cold Spring Harbor Laboratory Press; 2015–2017.
- 32.** Im K, Mareninov S, Diaz MFP, Yong WH. An introduction to performing immunofluorescence staining. *Methods Mol Biol.* 2019; 1897:299-311. doi: 10.1007/978-1-4939-8935-5\_26
- 33.** Tomasik P, Horton D. Enzymatic conversions of starch. *Adv Carbohydr Chem Biochem.* 2012; 68:59-436. doi: 10.1016/B978-0-12-396523-3.00001-4
- 34.** Slaoui M, Fiette L. Histopathology procedures: from tissue sampling to histopathological evaluation. *Methods Mol Biol.* 2011; 691:69-82. doi: 10.1007/978-1-60761-849-2\_4
- 35.** Chazotte B. Labeling nuclear DNA with hoechst 33342. *Cold Spring Harb Protoc.* 2011; 1:pdb.prot5557. doi: 10.1101/pdb.prot5557
- 36.** Duvernoy HM, Cattin F, Naidich TP, Raybaud C, Risold PY, Salvolini U, and Scarabine U. *The human hippocampus: functional anatomy, vascularization and serial sections with MRI,* 3rd edition. New York: Springer-Verlag; 2005.

## ANNEXES

### 1. HYPOTHESIZED PATHWAY OF THE ELIMINATION OF BRAIN WASTE SUBSTANCES THROUGH WASTEOSOMES

Wasteosomes (also known as *corpora amylacea*) are polyglucosan bodies that amass waste substances from different origins, including neuronal, glial and blood origin, and even from microbial and fungal infections (1). They are generated in astrocytes during normal aging and neurodegenerative processes, mostly in perivascular, periventricular and subpial regions (A). Wasteosomes are extruded from brain parenchyma to the CSF in the ventricles or subarachnoid space (2a and 2b) or to the perivascular space which is connected to the CSF via the glymphatic system (2c). Once in the CSF (3), they may enter the lymphatic capillaries of the subarachnoid space (4). Finally, they reach the cervical lymph nodes through the meningeal lymphatic vessels (5 and 6), and are phagocytised by macrophages, a process probably mediated by different paths (B) (7) (Fig. A).

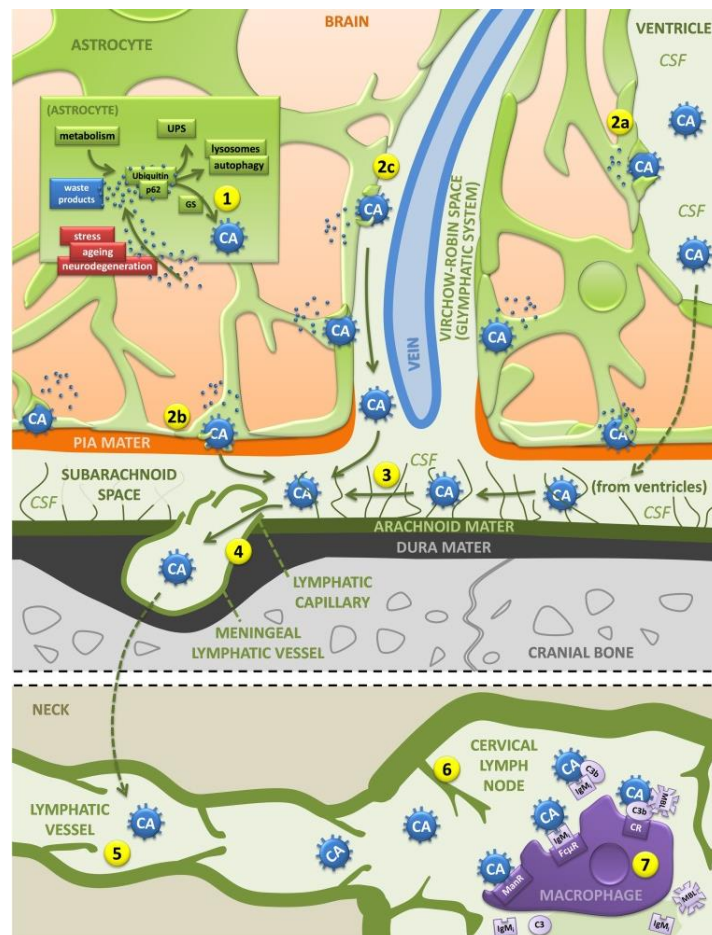


**Figure A:** Hypothesized pathway of the elimination of brain waste substances based on the role of wasteosomes as waste containers. CA, wasteosome (*corpora amylacea*); C3, C3 component of the complement system; C3b, C3b fragment generated from C3; CR, C3b receptor; ManR, mannose receptor; UPS, ubiquitin–proteasome system (B).

A recent study by Riba *et al.* has investigated the phagocytosis of wasteosomes *in vitro* using THP-1 macrophages. A time-lapse has shown how macrophages interact with wasteosomes, firstly extending a lamellipodium and afterwards engulfing the body to process it. Moreover, it has been noted that after phagocytosis of ConA labelled and AF555 NHS ester labelled wasteosomes, macrophages expose the fluorescent protein fraction of wasteosomes on their surface, as if they could act as antigen-presenting cells. Riba *et al.* also studied the phagocytic receptors on THP-1 macrophages that interact with wasteosomes. Results show THP-1 macrophages contain CD206 and CD35, but not the Fc receptor for IgM (also known as FAIM3). Nevertheless, the presence of FAIM3 should not be ruled out in other macrophage lines (C) (Fig. B). The CD206 (also known as Man receptor) is a C-lectin that recognises Man, GlcNAc and fucose residues, which may be present in wasteosomes (D,E). This lectin is expressed by M2 macrophages, known to be non-inflammatory macrophages (F), what makes sense to avoid unnecessary inflammatory responses in the processing of the waste substances of wasteosomes (C). The CD35 (also known as CR1 or C3b receptor) recognises C3b opsonizing protein (G). Opsonization of wasteosomes with C3b can happen through the lectin pathway, since wasteosomes could be targets of the Man-binding lectin (MBL) (H), and through the alternative pathway (I). MBL binds to Man and GlcNAc, whereas C3b generated by the spontaneous hydrolysis of C3 binds to Glc oligomers (H,I). The binding of MBL and C3b can be explained since both are found in the CSF (J,K). Bearing in mind wasteosomes could be opsonised with C3b once in the CSF, the study by Riba *et al.* focused also on phagocytosis *in vivo* at CNS interfaces, where there are perivascular, choroid plexus and meningeal macrophages (L). However, no macrophages with the CD35 were observed in these areas.

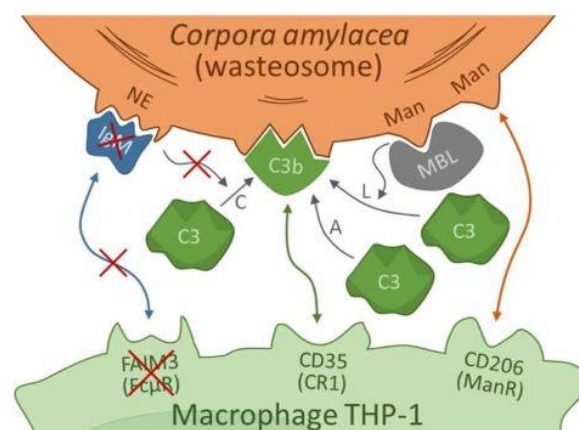


**Figure B:** Integrative scheme of the mechanisms involved in the phagocytosis of CSF wasteosomes by THP-1 macrophages. The absence of FAIM3 in THP-1 macrophages and the absence of IgM opsonizing the CSF wasteosomes (binding to their NE) indicate that the phagocytosis by THP-1 macrophages does not occur through the IgM-FAIM3. In addition, since there are no IgM opsonizing wasteosomes in the CSF, the opsonization with C3b in the CSF through the complement pathway is not possible in THP-1 macrophages. NE, neo-epitope; C3b, C3b fragment generated from C3; Man, mannose; IgM, antibody of immunoglobulin M class; C3, C3 component of the complement system; MBL, mannose-binding lectin; C, opsonization with C3b in the CSF through the complement pathway; A, opsonization with C3b in the CSF through the alternative pathway, triggered by the contact between C3 and wasteosomes; L, opsonization with C3b in the CSF through the lectin pathway, triggered by the binding of MBL with the wasteosomes; FAIM3, Fc receptor for IgM; CD35, CR1 or C3b receptor; CD206, mannose receptor (C).

## 2. THE NATURE OF THE NEO-EPITOPES

Regarding the composition of the NE, it is still indeterminate, although some studies suggest they are of carbohydrate nature (A,E). Humans have many NAb<sub>s</sub>, some of which belong to hIgM (M), that recognise glycan epitopes, such as advanced glycation end products, glycoproteins, and glycolipids (N,O,P,Q). The knowledge of carbohydrates still requires more study, but it is accepted they have multiple complex functions, which include acting as “eat-me signals” that may recruit macrophages (N,P). For instance, post-transcriptional modification of glycosylated lipids and proteins occurs during cancer development, generating “tumour-associated carbohydrate antigens”, although no matured specific Ab against a tumour has ever been detected (R,S). Such facts indicate not only peptides but also carbohydrates could play an important role as immune epitopes. Furthermore, a more recent study by Riba *et al.* showed preadsorption of hIgM with Glc, Man, fructose and GlcNAc reduced the interaction between these NAb<sub>s</sub> and wasteosomes, with Glc having the largest effect. Contrary, preadsorption of hIgM<sub>s</sub> with galactose and N-acetylgalactosamine, and digestion with pepsin had no effect on the staining. Such results rule out the possibility of the NE to be of glycoproteic nature and indicate that hIgM<sub>s</sub> recognise carbohydrate structures, some of which might be part of the NE of wasteosomes (E).

### 3. FEATURES OF OTHER AMYLOLITIC ENZYMES

Besides  $\gamma$ -amylase, there are other amylolytic enzymes which could be used for the study of biochemical features of wasteosomes. The characteristics of  $\alpha$ -amylase and  $\beta$ -amylase regarding their action mode when breaking  $\alpha$ -glycosidic linkages of polymerised hexoses are shown in [Table A](#) (A,T).

*Table A: Features of  $\alpha$ -amylase and  $\beta$ -amylase concerning the glycosidic linkages broken by their action, their breaking mode, the products released and their action blockers.*

<b>Enzyme</b>	<b>Glycosidic linkage broken</b>	<b>Breaking mode</b>	<b>Product</b>	<b>Action blocked by</b>
<b><math>\alpha</math>-amylase</b>	$\alpha$ -1:4 inside the macromolecule	rapidly, non-selectively and randomly	monosaccharides, disaccharides, oligosaccharides and dextrans	$\alpha$ -1:6 linkages
<b><math>\beta</math>-amylase</b>	$\alpha$ -1:4 at the outside end or nonreducing end of the polyglucosan	amylose chains of 6 Glc units, less efficient than $\alpha$ -amylase	maltose	$\alpha$ -1:6 linkages

## BIBLIOGRAPHY OF THE ANNEXES

- A.** Sakai M, Austin J, Witmer F, Trueb L. Studies of corpora amylacea: isolation and preliminary characterization by chemical and histochemical techniques. *Arch Neurol.* 1969; 21:526-44. doi: 10.1001/archneur.1969.00480170098011
- B.** Riba M, Augé E, Campo-Sabariz J, Moral-Anter D, Molina-Porcel L, Ximelis T, et al. Corpora amylacea act as containers that remove waste products from the brain. *Proc Natl Acad Sci USA.* 2019; 116:26038-26048. doi: 10.1073/pnas.1913741116
- C.** Riba M, Campo-Sabariz J, Tena I, Molina-Porcel L, Ximelis T, Calvo M, et al. Wasteosomes (corpora amylacea) of human brain are phagocytosed by non-inflammatory macrophages. Unpublished.
- D.** Feinberg H, Jégouzo SAF, Lasanajak Y, Smith DF, Drickamer K, Weis WI, et al. Structural analysis of carbohydrate binding by the macrophage mannose receptor CD206. *J Biol Chem.* 2021; 296:100368. doi: 10.1016/j.jbc.2021.100368
- E.** Riba M, Augé E, Tena I, Del Valle J, Molina-Porcel L, Ximelis T, et al. Corpora amylacea in the human brain exhibit neopeptides of a carbohydrate nature. *Front Immunol.* 2021; 12:618193. doi: 10.3389/fimmu.2021.618193
- F.** Shapouri-Moghaddam A, Mohammadian S, Vazini H, Taghadosi M, Esmaeili SA, Mardani F, et al. Macrophage plasticity, polarization, and function in health and disease. *J Cell Physiol.* 2018; 233:6425-6440. doi: 10.1002/jcp.26429
- G.** Smith BO, Mallin RL, Krych-Goldberg M, Wang X, Hauhart RE, Bromek K, et al. Structure of the C3b binding site of CR1 (CD35), the immune adherence receptor. *Cell.* 2002; 108:769-80. doi: 10.1016/s0092-8674(02)00672-4
- H.** Ip WK, Takahashi K, Ezekowitz RA, Stuart LM. Mannose-binding lectin and innate immunity. *Immunol Rev.* 2009; 230:9-21. doi: 10.1111/j.1600-065X.2009.00789.x
- I.** Pangburn MK. Analysis of recognition in the alternative pathway of complement. Effect of polysaccharide size. *J Immunol.* 1989; 142:2766-70.
- J.** Wu T, Dejanovic B, Gandham VD, Gogineni A, Edmonds R, Schauer S, et al. Complement C3 is activated in human AD brain and is required for neurodegeneration in mouse models of amyloidosis and tauopathy. *Cell Rep.* 2019; 28:2111-2123.e6. doi: 10.1016/j.celrep.2019.07.060
- K.** Reiber H, Padilla-Docal B, Jensenius JC, Dorta-Contreras AJ. Mannan-binding lectin in cerebrospinal fluid: a leptomeningeal protein. *Fluids Barriers CNS.* 2012; 9:17. doi: 10.1186/2045-8118-9-17
- L.** Kierdorf K, Masuda T, Jordão MJC, Prinz M. Macrophages at CNS interfaces: ontogeny and function in health and disease. *Nat Rev Neurosci.* [Internet]. 2019; 20:547-562. doi: 10.1038/s41583-019-0201-x
- M.** Xia L, Gildersleeve JC. Anti-glycan IgM repertoires in newborn human cord blood. *PLoS One.* 2019; 14:e0218575. doi: 10.1371/journal.pone.0218575
- N.** Grönwall C, Vas J, Silverman GJ. Protective roles of natural IgM antibodies. *Front Immunol.* 2012; 3:66. doi: 10.3389/fimmu.2012.00066
- O.** Maddur MS, Lacroix-Desmazes S, Dimitrov JD, Kazatchkine MD, Bayry J, Kaveri SV. Natural antibodies: from first-line defense against pathogens to perpetual immune homeostasis. *Clin Rev Allergy Immunol.* 2020; 58:213-228. doi: 10.1007/s12016-019-08746-9
- P.** Bovin NV. Natural antibodies to glycans. *Biochemistry (Mosc).* 2013; 78:786-97. doi: 10.1134/S0006297913070109
- Q.** Haji-Ghassemi O, Blackler RJ, Martin Young N, Evans SV. Antibody recognition of carbohydrate epitopes. *Glycobiology.* 2015; 25:920-52. doi: 10.1093/glycob/cwv037
- R.** Vollmers HP, Brändlein S. Natural IgM antibodies: the orphaned molecules in immune surveillance. *Adv Drug Deliv Rev.* 2006; 58:755-65. doi: 10.1016/j.addr.2005.08.007
- S.** Brändlein S, Pohle T, Ruoff N, Wozniak E, Müller-Hermelink HK, Vollmers HP. Natural IgM antibodies and immunosurveillance mechanisms against epithelial cancer cells in humans. *Cancer Res.* 2003; 63:7995-8005.
- T.** Tomasik P, Horton D. Enzymatic conversions of starch. *Adv Carbohydr Chem Biochem.* 2012; 68:59-436. doi: 10.1016/B978-0-12-396523-3.00001-4

